Low Temperature Physics/Fizika Nizkikh Temperatur, 2017, v. 43, No. 2, pp. 259–282

Spin resonance and spin fluctuations in a quantum wire

V.L. Pokrovsky

Department of Physics and Astronomy, Texas A&M University, College Station, TX 77843-4242

Landau Institute for Theoretical Physics, Chernogolovka, Moscow Distr. 142432, Russia
E-mail: valery@physics.tamu.edu

Received August 5, 2016, revised November 28, 2016, published online December 26, 2016

This is a review of theoretical works on spin resonance in a quantum wire associated with the spin-orbit interaction. We demonstrate that the spin-orbit induced internal "magnetic field" leads to a narrow spin-flip resonance at low temperatures in the absence of an applied magnetic field. An applied dc magnetic field perpendicular to and small compared with the spin-orbit field enhances the resonance absorption by several orders of magnitude. The component of applied field parallel to the spin-orbit field separates the resonance frequencies of right and left movers and enables a linearly polarized ac electric field to produce a dynamic magnetization as well as electric and spin currents. We start with a simple model of noninteracting electrons and then consider the interaction that is not weak in 1*d* electron system. We show that electron spin resonance in the spin-orbit field persists in the Luttinger liquid. The interaction produces an additional singularity (cusp) in the spin-flip channel associated with the plasma oscillation. As it was shown earlier by Starykh and his coworkers, the interacting 1*d* electron system in the external field with sufficiently large parallel component becomes unstable with respect to the appearance of a spin-density wave. This instability suppresses the spin resonance. The observation of the electron spin resonance in a thin wires requires low temperature and high intensity of electromagnetic field in the teraherz diapason. The experiment satisfying these two requirements is possible but rather difficult. An alternative approach that does not require strong ac field is to study two-time correlations of the total spin of the wire with an optical method developed by S.A. Crooker and coworkers. We developed theory of such correlations. We prove that the correlation of the total spin component parallel to the internal magnetic field is dominant in systems with the developed spin-density waves but it vanishes in Luttinger liquid. Thus, the measurement of spin correlations is a diagnostic tool to distinguish between the two states of electronic liquid in the quantum wire.

PACS: 73.21.Hb Quantum wires;
76.20.+q General theory of resonances and relaxations;
71.70.Ej Spin-orbit coupling, Zeeman and Stark splitting, Jahn–Teller effect.

Keywords: quantum wire, electron spin resonance, spin-orbit interaction, Luttinger liquid.

1. Introduction

In my youth I had a happiness and privilege to be a student with Professor Ilya Lifshitz, the great scientists and a brilliant personality. His influence on my life was rather deep, sometimes decisive. I am deeply obliged to our teachers and first of all to Ilya Mikhailovich who displayed fearlessness and uncompromiseness in all what concerned the science.

In this article dedicated to his memory I present a review on a topic associated with scientific interests of Ilya Mikhailovich: physical properties of extremely anisotropic materials, namely the so-called quantum wires (QW). Quantum wires are effectively one-dimensional systems that can be treated as waveguides for the de Broglie waves so narrow that only one mode propagates in it. It happens when the linear size of the wire cross section is about 1 nm. The QW can be created by special growth processes in which the wires appear suspended onto the relief of a substrate. Alternatively a narrow conducting channel can be created in a semiconductor film by applying a proper configuration of gate electrodes. In the beginning of the 21st century nanodevices have been engineered using the QW with predesigned properties [1–8]. These advances excited a new interest in comparatively weak electron interactions in nanowires, the most important weak spin-orbit interaction (SOI). The SOI is especially important in a media with violated reflection symmetry where it produces the momentum-dependent effective field acting on the electron spin known as Dresselhaus interaction [9]. Another important manifestation of the SOI proposed by Rashba [10,11] appears in thin films and wires due to the contact

with the interface that violates the reflection symmetry and is referred as Rashba interaction. Together they give a combined SOI-induced effective "magnetic" field linearly dependent on the electron momentum. In a QW the direction of this field does not vary and corresponding component of the total spin is conserved. In two and three dimensions all three components of the total spin are not conserved.

If the electron gas (liquid) is degenerate, low-energy electron-hole excitations play the dominant role in the processes induced by low-frequency electromagnetic field. In this situation the value of the electron momentum p in the SOI can be replaced in $1d$ systems by the Fermi-momentum p_F. Thus, the absolute value of the SOI field is determined in addition to its direction and it becomes a well-defined vector. The absolute value of the SOI field determines the resonance frequency of a new type of resonance, electronic spin resonance on the SOI field. We will call it inner resonance. Sometimes it is called chiral resonance. For two dimensions such a resonance was predicted by Shekhter *et al.* [12], but only in the case when Dresselhaus SOI is absent. This condition is not realistic. In the combined Dresselhaus–Rashba SOI the resonance frequency in two dimensions depends on momentum direction. It leads to the smearing of the inner resonance line. This smearing is absent in one-dimensional case.

The resonance frequency can be regulated by an external magnetic field $\mathbf{B}$. Its component $B_{\|}$ parallel to the SOI field creates difference between the resonance frequencies of the left and right movers and in this way the ac field induces direct electric and spin currents. The perpendicular component $B_{\perp}$ induces the electric dipolar mechanism of the spin-flip transitions instead of magnetic dipole acting in its absence. Since electric dipole is much more efficient for resonance absorption than magnetic ones, the resonance absorption grows very rapidly with $B_{\perp}$.

In Sec. 2 of this review we analyze the resonance phenomena employing a simple model of the ideal gas with SOI for electrons [13]. In Sec. 3 we consider a more realistic model of Luttinger liquid (LL) for electrons [14]. It is well known [15,16] that in $1d$ even a weak interaction destroys Fermi excitations in a vicinity of the Fermi point. Instead the collective Bose excitations — the charge and spin waves — play role of low-energy carriers of charge and spin, respectively. The SOI resonance can be treated as the excitation of a spin wave with the wave vector equal to the difference of the Fermi momenta for electrons with the same direction of the velocity but opposite directions of their spins. A new phenomenon caused by interaction together with the SOI is the appearance of a weak coupling between charge and spin channels and as a result the appearance of a new singularity (cusp) in the spin-flip response.

Usally experimenters observe the resonance attenuation of the electromagnetic wave. In the QW this experiment is difficult because it requires sufficiently low temperature to distinguish the split Fermi points and rather high power of the incident electromagnetic wave. The high power is necessary to enhance a weak signal from a not very big number of carriers in the wire. In a semiconductor wire of the length 10 μm with the bulk density of carriers 10^{18} cm^{-3} the number of electrons is about 1,000. The necessary power in the teraherz range is available only with free electron lasers. The necessary temperatures are in the He range. These rather exotic requirements can be avoided employing quite different experimental tool: the real-time measurement of the two-time correlators of the total electron spin of the wire proposed and realized by S.A. Crooker [17]. This method employs the Faraday rotation of the light polarization by magnetized sample. High sensitivity of this method allows to avoid large power of incident light beam. With this method it is possible to distinguish two competing states of the elctron liquid in the QW. One of these states is the LL. The second one was proposed by O.A. Starykh and his coworkers [18] is the static spin-density wave with the wave vector $2p_F$. They proved that it wins at sufficiently large ratio $B_{\|}/B_{\perp}$. We analyze the properties of the two-time spin correlators in the Sec. 4 of our review.

2. SOI spin resonance in ideal electron gas

In this section we consider electron spin resonance (ESR) in nanowires with SOI. It is based on the article [13]. For ESR in metals or semiconductors an applied magnetic field $\mathbf{B}$ splits the unique Fermi surface for both spin directions into two different Fermi surfaces for up and down spins, with the same Zeeman splitting for all electrons. An almost uniform applied ac field of frequency equal to the Zeeman energy then induces sharp transitions between states with the same momentum and opposite spin.

Even a weak SOI changes this picture. It creates an internal "magnetic field" $\mathbf{B}_{so}$ that depends linearly on the electron momentum for both Rashba and Dresselhaus SOI [9–11]. Therefore, for large enough SOI the ESR is smeared out. As indicated by Shekhter *et al.* [12], for 2D systems with only a Rashba interaction, the smearing is comparatively small at temperatures well below the Fermi energy, leading to a narrow ESR — a "chiral resonance". However, noted that simultaneous presence of both Rashba and Dresselhaus interactions smears out the resonance since the SOI resonance frequency ω_r depends on the 2D momentum direction.

This anisotropic broadening is completely absent for a QW (1D) as $\mathbf{B}_{so}$ has the same direction for all right-moving particles and the opposite direction for the left-movers. Since the Rashba–Dresselhaus SOI is much less than the Fermi energy, the spin-flip energy is well defined. Thus the ESR line is narrow at low temperatures. The spin-flip resonance adsorption in the wire in the absence of an applied magnetic field $\mathbf{B}$ is very weak since it is magnetic dipole induced. The main predictions of the theory of ESR

in free-electron systems with the SOI are: i) A component of **B** perpendicular to $\mathbf{B}_{so}$ activates electric dipole spin-flip transitions and therefore strongly enhances the resonance effects. Typically a **B** that is a tenth of $\mathbf{B}_{so}$ increases the resonance absorption by 4 orders of magnitude, while changing ω_r by only 1%. ii) The component of **B** parallel to $\mathbf{B}_{so}$ has little effect on the absorption, but it does separate the resonances of the right and left movers. Linearly polarized resonance radiation then produces a net magnetization and dc electric and spin currents.

The SOI-induced dipole spin-flip excitation in 2D by an ac electric field **E** polarized in plane was considered in Ref. 12. Since, because of the SOI, spins in 2D are not collinear the excitation probability is almost independent of **B**. Rashba and Efros [19] considered a similar problem, but with an ac **E** polarized perpendicularly to the plane. To ensure a narrow resonance in this system, **B** must significantly exceed $\mathbf{B}_{so}$. The authors concluded that a tilted **B** is necessary to activate the electric-field-spin interaction. Due to the very high symmetry of their system, their spin-flip probability is proportional to the 6th power of **B** (instead of the square, as in the present case). The resulting probability is very small for realistic field values.

In the following subsections we analyze the electronic spectrum and eigenstates with SOI included; the effective interaction of the electron spin with an ac electric field; the dynamic generation of steady-state currents and magnetization and the relaxation processes. In conclusion some numerical estimates are made.

2.1. Electronic spectrum and eigenstates

Weak SOI effects are better seen if the Fermi energy is not too large in comparison with the SOI energy. Therefore, it is reasonable to consider the SOI effects in semiconductors rather than in metals. Here we consider type III–V semiconductors and only their electron bands, to avoid complications associated with degeneracy of the hole band. In *p*-doped semiconductors, analogous effects of the same order of magnitude should occur for the light holes with $J = 3/2$ and $J_z = \pm 1/2$ similar to the present case of $S = 1/2$, $S_z = \pm 1/2$. But in the case of heavy holes with $J = 3/2$ and $J_z = \pm 3/2$ photons cannot cause transitions between the two states. The 1D electron density n is assumed to be sufficiently large and the temperature sufficiently low to ensure a degenerate Fermi gas.

In 1D the most general form of the SO interaction, including both Rashba and Dresselhaus terms, is $H_{so} = (\alpha\sigma_x + \beta\sigma_y)p$, where p is the 1D momentum along the wire direction x [20], and $\boldsymbol{\sigma}$ are the Pauli spin matrices. The total Hamiltonian, without impurity scattering, also includes the kinetic energy $p^2/2m^*$ and the Zeeman term $-\mathbf{b}\boldsymbol{\sigma}$, where $\mathbf{b} = g\mu_B\mathbf{B}/2$ has dimensionality of energy. Let us introduce a unit vector **n** in the direction $\alpha\hat{x} + \beta\hat{y}$ of B_{so} and define the longitudinal and transverse components of magnetic field: $\mathbf{b} = b_{\|}\mathbf{n} + \mathbf{b}_{\perp}$. With $\gamma \equiv \sqrt{\alpha^2 + \beta^2}$ the SO velocity, the total Hamiltonian then reads

$$H = p^2/2m^* + \left(\gamma p - b_{\|}\right)\mathbf{n}\boldsymbol{\sigma} - \mathbf{b}_{\perp}\boldsymbol{\sigma}. \tag{1}$$

Its eigenvalues are

$$E(p,\sigma) = p^2/2m^* + \sigma q, \tag{2}$$

where $q = \sqrt{(\gamma p - b_{\|})^2 + \mathbf{b}_{\perp}^2}$ and $\sigma = \pm 1$ gives the projection of the electron spin along the total effective magnetic field $\mathbf{B}_e \equiv \mathbf{B} + \mathbf{B}_{so}$ and is the eigenvalue of the operator

$$\Sigma = \frac{|\gamma p - b_{\|}|}{q}\left(\mathbf{n} - \frac{\mathbf{b}_{\perp}}{\gamma p - b_{\|}}\right)\boldsymbol{\sigma}. \tag{3}$$

For a nonzero transverse magnetic field $\mathbf{b}_{\perp}$, the direction of spin quantization depends on momentum. Figure 1 gives the energy *vs* magnetic field for small magnetic fields $|\mathbf{b}| << p_F^2/2m^*$, with two slightly distorted Rashba parabolas shifted vertically in opposite directions and an avoided crossing. The parallel component of the magnetic field $\mathbf{b}_{\|}$ causes the reflection asymmetry, whereas its perpendicular component $\mathbf{b}_{\perp}$ causes the avoided crossing of energy levels. The four Fermi momenta correspond to the left and right movers and the two values of σ.

For a typical experimental setup the SO velocity $\gamma << v_F = p_F/m^*$. If $|\mathbf{b}| << \gamma p_F$ then the four Fermi momenta differ only slightly from the Fermi momentum in the absence of SOI and applied magnetic field $\pm p_F = \pm\pi\hbar n/2$ and are given by

$$p_{\sigma\tau} = \tau p_F - \sigma m^*\left[\gamma - \tau\frac{b_{\|}}{p_F} + \frac{\mathbf{b}_{\perp}^2}{2p_F\left(\gamma p_F - \tau b_{\|}\right)}\right], \tag{4}$$

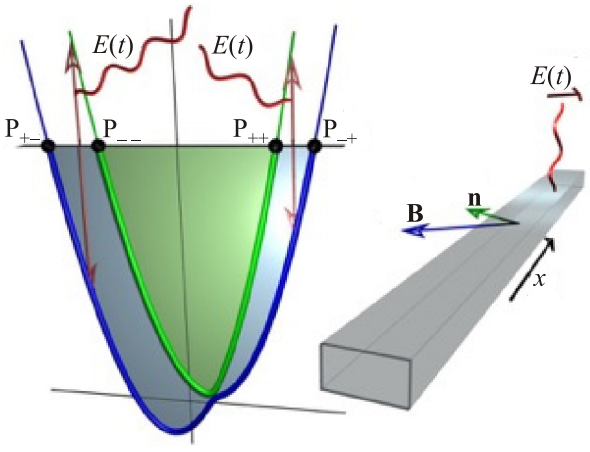

Fig. 1. (Color online) Left part: Energy *vs* momentum according to Eq. (1). Shadowed regions of the spectrum are occupied. The spin-flip excitations of the occupied states by ac electric field are shown by long vertical arrows. Right part: Geometry and directions of the applied magnetic field **B** and internal $\mathbf{B}_{so} \| \mathbf{n}$.

where $\tau = \pm 1$ indicates right (R) and left (L) movers. In the ground-state electrons with spin projection σ fill the momentum interval from $p_{\sigma-}$ to $p_{\sigma+}$.

All states in the interval (p_{--}, p_{++}) are doubly occupied. The states in the intervals (p_{++}, p_{-+}) and (p_{+-}, p_{--}) are singly occupied (Fig. 1). A net spin-flip is possible only in the singly occupied intervals and requires energy

$$E_{sf} = 2\left(\gamma \mid p \mid -\tau b_{\parallel}\right). \tag{5}$$

Thus, for $\mathbf{b}_{\parallel} \neq 0$, there are two different resonance frequencies corresponding to the right and left movers $\tau = \pm 1$. For $\gamma << v_F$, the spin-flip energies are centered at $E^0_{sf} = 2(\gamma p_F - \tau b_{\parallel})$ and lie in narrow bands of intrinsic width Δ, where

$$\Delta = 4m^*\gamma\left(\gamma - \tau b_{\parallel}/p_F\right) = 2\gamma E^0_{sf}/v_F << E^0_{sf}. \tag{6}$$

Spin-flip processes can be excited by a resonant applied field with frequency $\omega_r = E^0_{sf}/\hbar$. The temperature must satisfy $T < \hbar\omega_r/k_B$ to avoid thermal smearing.

2.2. Transition rate due to linearly polarized ac electric field

Let an ac field be linearly polarized along x:

$$E(t) = \hat{x}E_0(t)\mathrm{e}^{-i\omega_0 t} + \hat{x}E_0^*(t)\mathrm{e}^{i\omega_0 t} \tag{7}$$

and have spectral intensity $I(\omega)$ centered at ω_0 with extrinsic width $\Delta\omega << \omega_0$. The symbols $E_0(t)$ denote an envelope with frequencies in the interval $\Delta\omega$. Averaged over a time interval t' satisfying $2\pi/\omega_r << t' << \Delta\omega^{-1}$, the two-time correlator of field can be represented by an integral:

$$\overline{E_0^*(t)E_0(t')} = \frac{1}{2\pi}\int_{-\infty}^{\infty} I_\omega \mathrm{e}^{i\omega(t-t')}d\omega.$$

In the presence of electric and magnetic fields the momentum p in the Hamiltonian (1) must be replaced by $p + \frac{e}{c}A$, where A is the vector-potential. Thus, the SOI generates the spin dependence of the velocity:

$$v = \frac{c}{e}\frac{\partial H}{\partial A} = \frac{p + \frac{e}{c}A}{m^*} + \frac{\gamma e}{c}\sigma. \tag{8}$$

Here we used the Weyl gauge where the electric potential $\Phi = 0$, and thus

$$A = -\frac{ic}{\omega_0}\left(E_0(t)\mathrm{e}^{-i\omega_0 t} - E_0^*(t)\mathrm{e}^{i\omega_0 t}\right). \tag{9}$$

The interaction between the ac electric field and spin appears from the SOI term of the Hamiltonian. It reads

$$H_{\mathrm{int}} = -\frac{ie\gamma}{\omega_0}\left(E_0(t)\mathrm{e}^{-i\omega_0 t} - E_0^*(t)\mathrm{e}^{i\omega_0 t}\right)\mathbf{n}\boldsymbol{\sigma}. \tag{10}$$

For $\mathbf{b}_\perp = 0$, the interaction Hamiltonian is proportional to the same spin projection $\mathbf{n}\boldsymbol{\sigma}$ that enters Eq. (1), and therefore does not produce spin reversal. Then only magnetic dipole transitions can reverse the spin. Thus, there is no electric dipole contribution to the spin-flip transition in the absence of perpendicular component of the applied field $\mathbf{b}_\perp$.

This no-electric-dipole-spin-flip theorem was disputed by P. Upadhyaya *et al.* [21]. They noted that the SOI makes the magnetization and the internal "magnetic" field vary inside the wire in the direction perpendicular to its axis (x) and thus couple the electric field along y to the spin. However, in the article [13] we have found that to first and the second order in the small SOI parameter γ/v_F the contribution of this variation to the electric dipole coupling vanishes. The remaining, third order, coupling is comparable to or less than the magnetic dipole coupling and can be neglected. (See the details of our analysis in Appendix A.) This property is specific to 1D systems. In 2D the direction of $\mathbf{B}_e$ changes along with the momentum direction. Thus almost any spin interacts with a linearly polarized electric field.

In 1d the nonzero perpendicular component of the applied field $\mathbf{b}_\perp \neq 0$ couples the electric field with the spin and induces spin reversals exceeding the magnetic dipole spin reversal at rather small values of $b_\perp$. The matrix element $\langle + | \mathbf{n}\boldsymbol{\sigma} | - \rangle = 2|\mathbf{b}_\perp|/E^0_{sf}$ of the operator $\mathbf{n}\boldsymbol{\sigma}$ produces spin reversal between the two eigenstates of the operator Σ. Time-dependent perturbation theory gives that the spin-flip transition rate for an electron with momentum p is

$$w = \frac{4e^2\gamma^2}{\hbar^2\omega_0^2}(\mathbf{b}_\perp/E^0_{sf})^2 I_{(2\gamma|p|/\hbar)-\omega_0}.$$

On resonance, $I_\omega \approx 4\overline{E_0^2}/(\Delta\omega)$, which implies that

$$w \approx 4e^2\overline{E_0^2}\left(\mathbf{b}_\perp/E^0_{sf}\right)^2/p_F^2\Delta\omega. \tag{11}$$

The ratio of the electric and magnetic transition rates is $(c\mathbf{b}_\perp/v_F E^0_{sf})^2$. For InGaAs the ratio c/v_F is about 10^3. Thus, for $b_\perp \sim 10^{-1}E^0_{sf}$ the transition rate (11) exceeds the magnetic dipole induced rate by four orders, whereas the resonance frequency changes by only 1%.

The perturbation theory used above is valid if the average excited electron occupation number n_{ex} is small, i.e. $w\tau_{\mathrm{eff}} << 1$, where τ_{eff} is a characteristic lifetime. In the ballistic regime the time of flight $\tau_f = L/v_F$ plays the role of τ_{eff}. However, in 1D if the back-scattering time τ_b is much less than τ_f, then diffusion occurs, with lifetime $\tau_{\mathrm{eff}} = \tau_f^2/\tau_b >> \tau_f$. Saturation occurs for all excitation processes subject to recombination at a rate τ_{eff}^{-1}, $w\tau_{\mathrm{eff}} \gtrsim 1$, so the probability of excitation is $\min(w\tau_{\mathrm{eff}}, 1)$. For a narrow spectral width $\Delta\omega$, Rabi oscillations occur. The density of right-moving states subject to spin-resonant excitation is

$$n_{sr} = n\Delta\omega/4\omega_r. \tag{12}$$

2.3. Dynamic generation of permanent currents and magnetization

In the absence of applied longitudinal field the left movers with spin up and right movers with spin down have the same probability of spin-flip transition by ac field with the frequency close to the resonance. The resonance curves for both these groups of electrons are identical: they have rectangular shape with the width $8m\alpha^2$. The longitudinal field $b_\perp$ shifts energy of the spins by $-b_\parallel\sigma$. Thus, if $b_\parallel > 4m^*\gamma^2$, then the resonance lines for right and left movers do not overlap and can be excited separately. Thus a resonant linearly polarized ac field can produce a magnetization as well as steady-state electric and spin currents.

Consider a linearly polarized ac field that causes spin flips of right movers, so $n_{ex} = \delta n_{R\uparrow} = -\delta n_{R\downarrow}$. For electrons

$$n_{\rm ex} = \min(w\tau_{\rm eff},1)n_{sr}, \tag{13}$$

with equal hole density. The spin per electron is $s = n_{\rm ex}/n$. For $w\tau_{\rm eff} \geq 1$, $n_{\rm ex} = n_{sr}$. Thus, in the ballistic regime

$$j_e = -e(v_{R\uparrow}\delta n_{R\uparrow} + v_{R\downarrow}\delta n_{R\downarrow}) =$$

$$= -2\gamma e n_{\rm ex} = -enw\tau_f\gamma^2/v_F. \tag{14}$$

Next we consider how diffusion affects the currents. For simplicity we neglect spin-flip back-scattering and energy relaxation, but retain backscattering by impurities. A set of kinetic equations for this simplified model reads

$$dn^e_{R\uparrow}/dt = wn_{sr} - (\tau^{-1}_{\rm eff} + \tau_b^{-1})\delta n^e_{R\uparrow} + \tau_b^{-1}\delta n^e_{L\uparrow}, \tag{15}$$

$$dn^e_{L\uparrow}/dt = -(\tau^{-1}_{\rm eff} + \tau_b^{-1})\delta n^e_{L\uparrow} + \tau_b^{-1}\delta n^e_{R\uparrow}. \tag{16}$$

The ac field creates equal numbers of electrons and holes with parallel spins, and this property is maintained by the back-scattering if spin-flip processes are negligible. The pumped spin is polarized approximately along $\mathbf{n} + \mathbf{b}_\perp/\gamma p_F$. Its steady-state absolute value per unit length is $s_{\rm eff} = 2w\tau_{\rm eff}n_{sr}$. The spin current j_s is $j_s = g\mu_B v_F w n_{sr}\tau_{\rm eff}\tau_b/(2\tau_{\rm eff} + \tau_b)$. The electric current j_e is

$$j_e = -2e\gamma w n_{sr}\frac{\tau_{\rm eff}\tau_b}{2\tau_{\rm eff} + \tau_b} + ewn_{sr}\frac{b_\perp^2\tau_{\rm eff}(4\tau_{\rm eff} + \tau_b)}{\gamma p_F^2(2\tau_{\rm eff} + \tau_b)}. \tag{17}$$

Equation (17) shows that the electric current changes sign in the diffusive regime at $b_\perp = \gamma p_F\sqrt{\tau_b/2\tau_{\rm eff}}$. This happens because back-scattering equalizes the number of left and right moving excitations, whose velocities differ. For resonance of left movers, at frequency $\omega_r^L = 2(\gamma p_F + b_\parallel)/\hbar$, the magnetization and currents are reversed.

The generation of currents by an ac field is similar to the photogalvanic effect predicted by Ivchenko and Pikus [22] and by Belinicher [23]. More recently many clever modifications of this effect have been proposed and experimentally observed (see review [24], and articles [25,26]). They are mostly realized in 2D systems, but more importantly, unlike 1D, *nonresonant* optical or infrared radiation is used. In most cases, dynamic magnetization and electric current generation require a circularly polarized pumping field, whereas for a quantum wire in $\mathbf{B} \neq \mathbf{0}$ the same effect can be produced by a linearly polarized source. The 1D geometry implies a strong anisotropic dependence of the resonance line and transition probability on $\mathbf{B}$.

2.4. Relaxation processes

At low temperature the main mechanism for electron energy relaxation is phonon emission. If the corresponding relaxation time τ_{ep} becomes comparable to or less than τ_f, energy relaxation occurs before electrons and holes leave the wire. The total spin is not changed but the excitation velocities may decrease because lower energy means lower p and lower v. On the other hand, energy relaxation removes particles from the excited states and fills the depleted states. This makes an increase of power in the applied ac field more effective. The electron-phonon interaction is modeled by a standard Hamiltonian $H_{ep} = U\int \nabla\mathbf{u}(\mathbf{x})\psi^\dagger(\mathbf{x})\psi(\mathbf{x})$, where $\mathbf{u}(\mathbf{x})$ is the displacement vector, $\psi(\mathbf{x})$ is the electron field operator and U is the deformation potential. Electrons in the wire are always 1D, but phonons can be 1D, 2D, or 3D depending on the experimental setup. Let M and a be the lattice cell mass and lattice constant, and let u be the sound velocity. Then for an electron with momentum deviating by ξ from the Fermi point, and emitting 3D phonons, the relaxation rate is

$$\tau_{ep}^{-1} = \frac{U^2}{6\pi\hbar Muv_F}\left(\frac{v_F\xi a}{u\hbar}\right)^3. \tag{18}$$

The detailed calculation can be found in the Appendix to the article [13].

Thus, even at such high density of energy, the dc electric current through the QW is rather weak and magnetization per electron is small. Though the absolute value of the dc current is small, its density is large enough: 2,000 A/cm^2 for the current 1 nA.

In 2D and 3D systems elastic scattering (diffusion) leads to spin relaxation by the Dyakonov–Perel mechanism [27,28] because the direction of $\mathbf{B}_{so}$ depends on the direction of the $\mathbf{p}$ and is randomized by diffusion. In 1D for $\mathbf{b}_\perp = 0$ the direction of $\mathbf{B}_{so}$ is the same for all electrons, so the Dyakonov–Perel mechanism does not apply. A suppression of Dyakonov–Perel relaxation in 1D was found in numerical calculations [29]. However, for $\mathbf{b}_\perp \neq 0$, spin flip does occur in back-scattering, but its probability is of the order of $(\mathbf{b}_\perp/E^0_{sf})^2$ and can be neglected.

Other spin relaxation mechanisms, such as phonon emission combined with SOI, are much weaker.

2.5. Numerical estimates

All numerical estimates are for $In_{0.53}Ga_{0.47}As$. We take $m^* = 4.3\cdot10^{-29}$ g $\approx 0.05m_e$, $\alpha = 1.08\cdot10^6$ cm/s, and $g = -0.5$ [30–32]. A typical 2D electron density is $2\cdot10^{12}$ g·cm^{-2}. Take wire thickness $a = 5$ nm and width $d = 10$ nm. Then we find 1D density $n = 10^6$ cm^{-1}, $p_F = 1.65\cdot10^{-21}$ g·cm/s and $v_F = 0.38\cdot10^8$ cm/s. Assuming $\alpha = \beta$, we have $\omega_r = 4.8\cdot10^{12}$ s^{-1} (~ 0.8 THz) and intrinsic width $\delta = \Delta/\hbar \approx 3.8\cdot10^{11}$ s^{-1}. The value $\overline{E_0^2}$ in Eq. (11) is determined by the source power in the terahertz range. Although standard cascade lasers have power in the range 1 mW–1 W [33,34], the power can be strongly enhanced by non-linear devices, and in very short pulses (1 ps) it can reach 1 MW [35–38]. The free-electron laser at UCSB provides a continuous power of 1–6 kW for the frequency range 0.9–4.75 THz. On focusing, the energy flux rises to 40 kW/cm^2 [38]. For the moderate flux $S = 1$ kW/cm^2, we find $\overline{E_0^2} = 4\pi S/c = 4.19$ erg/cm^3. For $B_\perp = 10$ T we have $b_\perp/E_{sf}^0 = 0.05$, and Eq. (11) yields $w = 0.92\cdot10^{10}$ s^{-1}. As noted above, w can be increased by changing the power or the focus area. For length $L = 1-10$ μm the time of flight is $\tau_f = 2.6\cdot(10^{-12}–10^{-11})$ s. The backscattering time τ_b can be estimated from typical mobilities $\mu = e\tau/m^* = 2\cdot10^4–4\cdot10^5$ cm^2/(V·s) in the bulk or film [39]. Since the scattering cross-section area is much less than the wire cross-section area, τ can be identified with τ_b. Typical values are $\tau_b = 5\cdot10^{-13}–10^{-11}$ s. In this case the regime is either diffusive or marginally diffusive-ballistic.

First consider a ballistic regime with $\tau_f = 1.1\cdot10^{-11}$ s. By Eq. (14) the electric current equals 1 nA. The ratio of spin current to the electric current in units of elementary charges per second is $v_f/(2\gamma) \approx 12$. The magnetization per electron, in Bohr magnetons, is $(n_{sr}/n)w\tau_{\text{eff}} \sim 0.004$. Now consider a diffusive regime with $\tau_b = 1.1\cdot10^{-12}$ s and $\tau_f = 1.1\cdot10^{-11}$ s, so $\tau_{\text{eff}} = 1.1\cdot10^{-10}$ s. By Eq. (17) the electric current is $I = j_e = 0.12$ nA and the magnetization per electron is $0.02\,\mu_B$. The temperature must be maintained below $2\gamma p_F/k_B \approx 35$ K. $w\tau_{\text{eff}}$ in this case is approximately 1, indicating that saturation has been attained. For energy relaxation we assume 3D phonons. For InGaAs we take U = 16 eV, $u = 3.3\cdot10^5$ cm/s [40], $a = 5$ Å, $M = 1.8\cdot10^{-22}$ g and $\xi = m^*\gamma$. Then by Eq. (8) $\tau_{ep} = 1.4\cdot10^{-12}$ s. With 2D and 1D phonons the formulae differ, but numerical estimates give the same order of magnitude. This result shows that, even in the ballistic regime, τ_{ep} is usually much shorter than τ_f, so energy relaxation is substantial, which decreases the currents.

3. SOI-induced resonance in Luttinger liquids

In previous section we considered electron system in a QW as an ideal Fermi gas. However, in 1D systems the electron-electron interaction is known to be strong $V/\varepsilon_F \sim |\ln(na)|/(na)$, where ε_F is the Fermi energy, n is the 1D electron density, $a = \hbar^2\kappa/(me^2)$ is the Bohr's radius in the material, $m = 0.05m_e$ is the effective electron mass, and κ is the dielectric constant. For typical values $n \sim 10^6$ cm^{-1} and $\kappa \sim 20$ the ratio $V/\varepsilon_F \simeq 1$. Therefore, it is important to study the effect of interaction on electron spin resonance in a quantum wire with the SOI. In the present section we demonstrate that the resonance persists despite of disappearance of fermionic excitations. The ESR in the Luttinger electron liquid is the excitation of a spin wave by external ac electromagnetic field. This resonance would have a simple Lorentzian shape in the absence of interaction.

As we mentioned earlier, the fermionic excitation does not exist in the Luttinger liquid. They are replaced by bosonic excitations: charge and spin waves [15,16]. The standard Luttinger liquid (LL) theory neglects the SOI and deviation of the electronic spectrum near the Fermi points from the linear behavior. In this approximation the charge and spin degrees of freedom do not interact (this is the so-called spin-charge separation). The SOI splits the Fermi points for different spin projections and makes possible the resonant spin-flip processes. It was shown that the interplay of magnetic field, SOI, and electron-electron interaction leads to the formation of spin-density wave state when magnetic field is perpendicular to the effective SOI magnetic field [18]. In this section we assume that the magnetic field has nonzero component along the SOI field. Such a field terminates the spin-density wave instability and simultaneously separates the spin resonances for left and right movers (see the previous section). The Coulomb interaction in the Luttinger liquid usually changes the shape of the spin resonance line from simple Lorentzian to a power-like one [15,16]. but it does not violate spin-charge separation. It is the SOI that violates spin-charge separation and thus enables the excitation of the charge waves at spin reversal. This process be experimentally observed as a weak resonance (cusp) at a plasmon frequency instead of the spin-wave frequency. In this section we show that both these effects really take place, though both are weak for not too strong electron-electron interaction.

3.1. Model Hamiltonian

To take in account simultaneously the Coulomb interaction, SOI and external magnetic field, we use a model fermionic Hamiltonian:

$$H = H_{TL} + H_R + H_Z. \tag{19}$$

Here H_{TL} is the standard Tomonaga–Luttinger Hamiltonian:

$$H_{TL} = -iv_F \sum_{\sigma} \int dx(\psi^{\dagger}_{R,\sigma}\partial_x\psi_{R,\sigma} - \psi^{\dagger}_{L,\sigma}\partial_x\psi_{L,\sigma}) +$$

$$+ G\sum_{\sigma,\tau}\int dx\left[\rho_{\sigma,\tau}(x)\right]^2. \qquad (20)$$

The first term in the r.h.s. of this equation is the kinetic energy, the second term is the interaction between electrons. Approximation accepted in Eq. (20) neglects the quadratic correction to the kinetic energy of an electron near the Fermi point and replaces the long-range Coulomb interaction by a short-range interaction with G being the interaction constant. The summation index σ corresponds to the spin of electrons, the index $\tau = L, R$ corresponds to the left or right movers. The Hamiltonian H_{TL} is invariant with respect to the group of rotations $SU(2)$ in the spin space. The spin-orbit (Rashba) Hamiltonian H_R reads as follows [10]:

$$H_R = \alpha\int \psi^{\dagger} p_x\sigma_z\psi dx. \qquad (21)$$

The Rashba SOI splits Fermi momenta of up and down spins so that four Fermi points $p_{\rho,\sigma} = \rho p_F - \sigma\alpha m$ appear, but it leaves Fermi velocities unchanged. The Rashba SOI constant α has dimensionality of velocity and we assume $\alpha << v_F$; σ_z is the Pauli matrix; p_F is the Fermi momentum at $\alpha = 0$; and $\rho, \sigma = \pm 1$ correspond to right (left) movers and up (down) spin projections, respectively. Though for brevity we speak about Rashba interaction, the Hamiltonian H_R can include the Dresselhaus interaction as well. The only modification that the reader should have in mind is that the direction $\hat{z}$ in the pure Rashba interaction is perpendicular to the wire, whereas in combined Rashba–Dresselhaus interaction this direction is tilted to the wire at some fixed angle different from 90°. In the absence of external magnetic field the Fermi-momenta splitting can be removed by a single-particle unitary transformation $U = \exp(-i\sigma_z\alpha m x/\hbar)$ which shifts the momenta by $\pm\alpha m$. After this transformation the electronic spectrum becomes the same as without the SOI and the $SU(2)$ symmetry is restored.

An external permanent magnetic field breaks this symmetry. It leads to additional splitting of the Fermi points and to a difference in Fermi velocities for up and down spins, which cannot be compensated by this unitary transformation. We consider in this article only the magnetic field, $B_{\perp}$, perpendicular to the Rashba field (along z axis) and apply it for definiteness along x axis. The longitudinal field $B_{\|}$ destroys spin-density wave when its magnitude (in energy units) is much larger than the width of the spin resonance $4m\alpha^2$ [18]. The latter value is much smaller than the resonance frequency $2\alpha p_F$. Therefore, it is possible to destroy SDW and still have resonance frequency very close to $2\alpha p_F$, i.e., to neglect $B_{\|}$ in all following equations. Thus, the Zeeman Hamiltonian reads

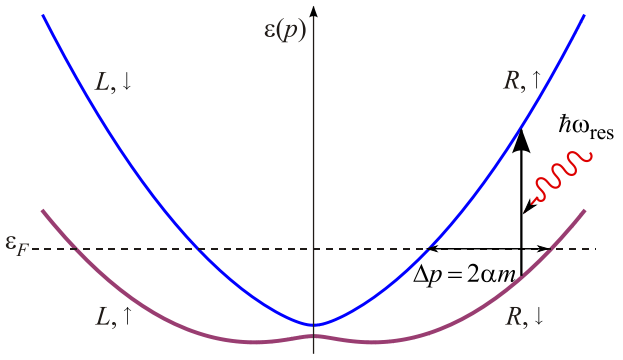

Fig. 2. (Color online) The up-spin and down-spin branches of the electron spectrum with nonzero Rashba spin-orbit interaction α and magnetic field $B_{\perp}$.

$$H_Z = -\frac{g\mu_B B_{\perp}}{2}\sum_{\rho,\sigma,\sigma'}\int dx\psi^{\dagger}_{\rho\sigma}(\sigma_x)_{\sigma\sigma'}\psi_{\rho\sigma'}, \qquad (22)$$

Further we consider the effect of the $SU(2)$ violation by external magnetic field employing perturbation theory. Therefore it is convenient to divide the total Hamiltonian (19) into the $SU(2)$-invariant part $H_0 = H_{TL} + H_R$ and the perturbation. Moroz *et al.* [41,42] have shown that a velocity difference $\delta v = v_{R,\uparrow} - v_{R,\downarrow} = v_{L,\downarrow} - v_{L,\uparrow}$ appears also due to the Rashba SOI in the wires of finite width. The curvature of the bands near Fermi level [43–48] can also be effectively taken into account by the nonzero velocity difference δv on the upper and lower branches of the energy spectrum. The later effect has a relative value of at most $\sim \alpha / v_F$. Figure 2 schematically shows the electron energy as a function of momentum in the presence of the transverse magnetic field.

We assume that the magnetic field is weak, $g\mu_B B_{\perp} << \alpha p_F$, and further consider it perturbatively. The residual symmetry in the perpendicular field is the combined reflection $p, \sigma \to -p, -\sigma$. It ensures that the right movers with the spin projection σ along z axis have the same velocity as the left movers with the same energy and the opposite spin projection $v_{R,\sigma} = v_{L,-\sigma}$, but $v_{R,\sigma} \neq v_{R,-\sigma}$.

3.2. Resonant absorption at spin-flip in the LL

To calculate the resonant absorption at SOI resonance in the LL we start with the Hamiltonian H_{em} of the interaction between the ac electromagnetic field and electrons. It can be found in many different textbooks, for example [50]:

$$H_{em} = -\frac{1}{c}\int jA_x dx, \qquad (23)$$

where $j = e\psi^{\dagger}(x)\hat{v}\psi(x)$ is the current, $\hat{v} = \hat{p}/m + \alpha\sigma_z$ is the velocity operator, and A_x denotes the x component of the vector potential of the ac field. As in the Sec. 2 we em-

ploy the Coulomb gauge, $\mathbf{A} = 0$ and put the scalar potential zero. In this gauge the electric field is $\mathbf{E} = -(1/c)\partial\mathbf{A}/\partial t$. The part of the electric current responsible for the spin-flip processes is

$$j_s(x) = e\alpha\psi^\dagger(x)\sigma_z\psi(x). \tag{24}$$

The absorption power of electromagnetic field is determined by the real part of the conductivity σ_ω at the frequency ω of the field multiplied by the square of the field's amplitude $|E_x(\omega)|^2$. We employ the Kubo formula for the conductivity:

$$\sigma_\omega = -\frac{1}{\hbar\omega l}\int_0^l dx\int_0^l dx'\int_{-\infty}^{\infty} dt'\theta(t-t')e^{i\omega(t-t')}\times$$

$$\times\langle[j_s(x,t), j_s(x',t')]\rangle, \tag{25}$$

where l is the length of the wire. According to Eq. (24), $j_s(x)$ is proportional to the density of z component of the spin. Therefore, the spin-flip conductivity (25) can be represented as

$$\sigma_\omega = -\frac{4(e\alpha)^2}{\hbar\omega l}\int_{-\infty}^{t}\langle[S_z(t), S_z(t')]\rangle e^{i\omega(t-t')}dt', \tag{26}$$

where $S_z(t)$ is the operator of the total spin projection at the moment of time t. In the absence of magnetic field $B_\perp$ the z component of the total spin is conserved. Therefore, $[S_z(t), S_z(t')] = 0$ and the conductivity associated with the spin flip is zero. The violation of this conservation law at small $B_\perp$ in the first-order approximation of the time-dependent perturbation theory leads to

$$\delta S_z(t) = -\frac{i}{\hbar}\int_{-\infty}^{t}[V_I(t'), S_z(t')]dt', \tag{27}$$

where $V_I(t) = U_0^{-1}(t)(-g\mu_B B_\perp S_x)U_0(t)$ with $U_0(t) = \exp(-iH_0 t/\hbar)$ being the evolution operator in the absence of magnetic field, and S_x is the projection of the total spin on the x axis. It is convenient to write the Rashba Hamiltonian as a sum over electrons: $H_R = \sum_i \alpha p_i \sigma_{z,i}$. The kinetic and interaction energies commute with S_x, and therefore the perturbation operator $V_I(t)$ becomes

$$V_I(t) = -\frac{g\mu_B B_\perp}{2}\sum_i\left(\sigma_{x,i}\cos\omega_i t + \sigma_{y,i}\sin\omega_i t\right),$$

where $\omega_i = 2\alpha p_i/\hbar$. Substituting this expression into Eq. (27), we obtain

$$\delta S_z = \frac{g\mu_B B_\perp}{2\alpha}\sum_i\frac{1}{p_i}\left(\sigma_{+,i}e^{-i\omega_i t} + \sigma_{-,i}e^{i\omega_i t}\right), \tag{28}$$

where $\sigma_\pm = \sigma_x \pm i\sigma_y$. Condition $\alpha << v_F$ makes it possible to replace the factor $1/p_i$ in Eq. (28) by $\pm 1/p_F$. Then the expression for δS_z becomes proportional to the sum of the operators $\sigma_{\pm,i}(t) = \sigma_{\pm,i}\exp(\mp i\omega t)$. In terms of secondary quantized operators it reads (we keep here only right movers):

$$\delta S_z(t) = \frac{g\mu_B B_\perp}{2\alpha p_F}\int\psi^\dagger_{R,\uparrow}(x,t)\psi_{R,\downarrow}(x,t)dx + \text{h.c.} \tag{29}$$

The unitary transformation $U = \exp(-i\sigma_z\alpha mx/\hbar)$ that puts the split Fermi points together, modifies this equation by multiplying the integrand by factor $\exp(-2i\alpha mx/\hbar)$. As a result, we find for the conductivity (25) associated with the spin flip [51],

$$\sigma_\omega = -\frac{(eg\mu_B B_\perp)^2}{\hbar\omega l p_F^2}\int_0^l dx\int_0^l dx'\int_{-\infty}^{\infty} dt'\theta(t-t')e^{i\omega(t-t')}\times$$

$$\times\langle[\psi^\dagger_{R,\uparrow}(x,t)\psi_{R,\downarrow}(x,t), \psi^\dagger_{R,\downarrow}(x',t')\psi_{R,\uparrow}(x',t')]\rangle\times$$

$$\times e^{-2i\alpha m(x-x')/\hbar}. \tag{30}$$

This expression for spin-flip conductivity is the basic for the following calculation. It is convenient since the average of four fermions in it must be calculated for the Hamiltonian H_0. A little its modification taking in account a weak violation of $SU(2)$ symmetry by the SOI will be discussed later.

3.3. Bosonization

The particles propagating in a narrow channel in one direction with the same or close velocities interact a long time. Therefore, the interaction is not weak for fermions, whereas their collective excitations do not interact. The transformation from fermion to boson operators in 1d called bosonization was proposed in 1975 independently by elementary particle physicists S. Coleman and S. Mandelstam and by condensed matter theorists A. Luther and D. Mattis. It was repeatedly presented in numerous books and reviews. The standard and most informative references are already cited books [15,16]. The standard expression of fermionic operators in terms of bosonic operators reads

$$\psi_{\rho,\sigma} = U_{\rho,\sigma}\frac{e^{i\rho k_F x}}{\sqrt{2\pi a_0}}e^{-i[\rho\varphi_c(x) - \theta_c(x) + \rho\sigma\varphi_s(x) - \sigma\theta_s(x)]/\sqrt{2}}, \tag{31}$$

where $U_{\rho,\sigma}$ are the Klein factors which ensure the proper anticommutation relations between the fermion, and a_0 is the ultraviolet cutoff length. The secondary quantized fermionic wave functions ψ_σ can be represented by the linear combinations of right-moving and left-moving fermions $\psi_{\rho,\sigma}$ with the momenta being close to $\pm k_F$, i.e., $\psi_\sigma = \psi_{R,\sigma} + \psi_{L,\sigma}$. The advantage of this model is that the interaction energy becomes quadratic in the charge and spin density bosonic operators. The density of fermions becomes linear in bosonic fields $\varphi_{c,s}$,

$$\rho_{c,s}(x) = -\frac{\sqrt{2}}{\pi}\partial_x \varphi_{c,s}(x). \quad (32)$$

As we have seen already, the SOI leaves the velocities at four Fermi points equal in linear approximation, but the quadratic corrections make velocities of inner Fermi points different from the velocities of outer ones. After the canonical transformation inner and outer Fermi points merge, however the velocities all are different. Let they are v_1 and v_2. Then the kinetic energy should be modified in comparison to that in Eq. (20):

$$H_{\rm kin} = -iv_1 \int dx(\psi^\dagger_{R,\uparrow}\partial_x \psi_{R,\uparrow} - \psi^\dagger_{L,\downarrow}\partial_x \psi_{L,\downarrow}) -$$

$$-iv_2 \int dx(\psi^\dagger_{R,\downarrow}\partial_x \psi_{R,\downarrow} - \psi^\dagger_{L,\uparrow}\partial_x \psi_{L,\uparrow}). \quad (33)$$

This simple modification of the Luttinger Hamiltonian was proposed by Moroz *et al.* [41,42]. A difference of velocities $\delta v = v_1 - v_2$ appears not only due to quadratic part of dispersion, but also due to the SOI effect in a wire of finite thickness [14,41,42]. After bosonization the total Hamiltonian with kinetic energy given by Eq. (33) takes the form

$$H = \int \frac{dx}{2\pi}\left[v_c K_c \left(\partial_x \theta_c\right)^2 + \frac{v_c}{K_c}\left(\partial_x \varphi_c\right)^2 + v_s K_s \left(\partial_x \theta_s\right)^2 + \right.$$

$$\left. + \frac{v_s}{K_s}\left(\partial_x \varphi_s\right)^2 + \delta v\left(\partial_x \varphi_c \partial_x \theta_s + \partial_x \varphi_s \partial_x \theta_c\right)\right], \quad (34)$$

where v_c (v_s) is the velocity of plasmons (spinons). We have omitted the term $\int \cos[2\sqrt{2}\varphi_s(x)]dx/(2\pi)$ as being irrelevant in the renormalization group procedure for the repulsive interactions ($K_c < 1$) [42]. The reader is advised to find the derivation of the main part of the Hamiltonian (34) in the cited books on bosonization. The correction proportional to δv directly follows from bosonization transformation Eq. (31).

3.4. Spin resonance as spin-wave excitation

The bosonization allows us to consider the SOI resonance as the spin-wave excitation. To find the conductivity (30) we need to calculate the retarded correlation function

$$I^R_{\uparrow\downarrow,\downarrow\uparrow}(x,t) =$$

$$= -i\theta(t)\langle[\psi^\dagger_{R,\uparrow}(x,t)\psi_{R,\downarrow}(x,t), \psi^\dagger_{R,\downarrow}(0,0)\psi_{R,\uparrow}(0,0)]\rangle$$

in the ground state of the Hamiltonian (34) with fermionic operators $\psi_{\rho\sigma}$ given by Eq. (31). Since the perturbation theory is developed for time-ordered averages in the imaginary time $\tau = -it$ [52], it is necessary to express $I^R(x,t)$ in the Kubo formula (30) to the time-ordered product

$$I^T_{\uparrow\downarrow,\downarrow\uparrow}(x,\tau) = -\langle T_\tau \psi^\dagger_{R\uparrow}(x,\tau)\psi_{R\downarrow}(x,\tau)\psi^\dagger_{R\downarrow}(0,0)\psi_{R\uparrow}(0,0)\rangle.$$

Applying the Wick theorem, we obtain in terms of bosonic operators:

$$I^T_{\uparrow\downarrow,\downarrow\uparrow}(x,\tau) \propto -\frac{e^{g(x,\tau)}}{(2\pi a_0)^2},$$

$$g(x,\tau) = \sum_{q,\omega}[1 - e^{i(\omega\tau - qx)}]\langle Y(q,\omega)Y(-q,-\omega)\rangle, \quad (35)$$

where we introduced $e^{Y(x,\tau)}/(2\pi a_0) = \psi^\dagger_{R\uparrow}(x,\tau)\psi_{R\downarrow}(x,\tau)$ so that $Y(x,\tau) = i\sqrt{2}[\varphi_s(x,\tau) - \theta_s(x,\tau)]$ and $\tau > 0$. After obtaining $I^T_{\uparrow\downarrow,\downarrow\uparrow}(x,\tau)$, it can be converted into retarded correlator using $I^R_{\uparrow\downarrow,\downarrow\uparrow}(t) = i\theta(t)[I^T_{\uparrow\downarrow,\downarrow\uparrow}(t) - (I^T_{\downarrow\uparrow,\uparrow\downarrow}(-t))^*]$ [15]. Using standard techniques one can calculate the time-ordered fermionic correlation function in real time, see the Appendix B for the details of calculation of time-ordered fermionic correlation function in real time. It can be converted into retarded correlation function as $I^R_{\uparrow\downarrow,\downarrow\uparrow}(t) = -2\theta(t)\mathrm{Im}I^T_{\uparrow\downarrow,\downarrow\uparrow}(t)$, as shown in the Appendix C, and using Eq. (30) we obtain

$$\sigma_\omega = \mathcal{A}\int_{-\infty}^{\infty} dx \int_0^\infty e^{i(\omega t - qx)}[K(t+i\delta) - K(t-i\delta)]dt, \quad (36)$$

$$K(t) = \frac{1}{(x - v_c t)^\lambda (x + v_c t)^\mu (x - v_s t)^\nu}, \quad (37)$$

where the constant

$$\mathcal{A} = \frac{(eg\mu_B B_\perp)^2 a_0^{\lambda+\mu+\nu-2}}{2\pi^2 p_F^3 \alpha}. \quad (38)$$

We recall that the wave vector q in the above integral is equal to $2\alpha m/\hbar$, cf. Eq. (30). The exact numerical factor $\mathcal{A}$ is obtained here from the comparison with the non-interacting result of Ref. 13. The integrand in the integral over x has two singularities in the lower half-plane, at $x = v_s t$ and $x = v_c t$. The expressions for the exponents λ, μ, and ν are as follows [53]:

$$\lambda = (\delta v)^2 \frac{(1+K_c)^2}{8K_c(v_c - v_s)^2}, \quad (39)$$

$$\mu = (\delta v)^2 \frac{(K_c - 1)^2}{8K_c(v_c + v_s)^2}, \quad (40)$$

$$\nu = 2 - (\delta v)^2 \frac{K_c v_c^2 + (K_c^2 + 1)v_c v_s + K_c v_s^2}{2K_c(v_c^2 - v_s^2)^2}. \quad (41)$$

To approximate σ_ω close to the spin resonance at frequency $\omega_{\rm res} = v_s q = 2\alpha m v_s/\hbar$, we take $\gamma \le |\omega - \omega_{\rm res}| << \omega_{\rm res}$ with γ being the width of the resonance which we assume

to be small. In the limit $(v_c - v_s)\omega_{\rm res}/(v_s\gamma) >> 1$, it is calculated in the Appendix D and given by

$$\mathrm{Re}\ \sigma_\omega \simeq \mathcal{A}\frac{q^{\nu-1}}{(v_c-v_s)^\lambda (v_c+v_s)^\mu \Gamma(\nu)}\times$$

$$\times \frac{\gamma}{\left[(\omega-\omega_{\rm res})^2+\gamma^2\right]^{1-\frac{\lambda+\mu}{2}}}. \qquad (42)$$

Physically Eq. (42) indicates that the chosen momentum of the spin wave excited by the electromagnetic field, $2\alpha m/\hbar$, is associated with the spin-dependent translation in the momentum space needed to put together two SOI-split parabolas, see Fig. 2. This momentum defines the frequency of the excited spin wave. In the absence of SOI this momentum is zero and there is no ESR.

To evaluate σ_ω close to the other singularity, $\omega = 2\alpha m v_c/\hbar$, we use a similar approximation and obtain

$$\mathrm{Re}\ \sigma_\omega \simeq \mathcal{A}\frac{2\pi\lambda q^{\lambda-1}}{(2v_c)^\mu (v_c-v_s)^\nu (2-\mu-\nu)}\times$$

$$\times \frac{\gamma}{\left[(\omega-v_c q)^2+\gamma^2\right]^{1-\frac{\mu+\nu}{2}}}. \qquad (43)$$

The plasmon singularity has a character of a weak cusp that can be detected only at nonzero interaction. Physically Eq. (43) indicates that the spin-charge coupling in the presence of SOI is responsible for this cusp. Experimentally, even at weak interactions, the plasmon cusp can be resolved if the maximal derivative of Eq. (43) with respect to frequency is larger than the derivative of Eq. (42) at the same frequency. This condition is satisfied near the plasmon cusp if $(\delta v)^2(v_c q - \omega_{\rm res})/\gamma < 1$.

Equations (42) and (43) are obtained under the assumption of well separated spinon and plasmon peaks, $(v_c - v_s)q >> \gamma$ [54]. In the opposite case corresponding to the limit of noninteracting fermions, the peaks at $\omega = \omega_{\rm res}$ and $\omega = v_c q$ merge. According to Eq. (36), the combined power of the merged peaks is

$$\lambda + \nu = 2 + (\delta v)^2 (1-K_c)^2/[8K_c(v_c+v_s)^2].$$

In the limit of noninteracting fermions $v_c \to v_s$ and $K_c \to 1$, so that the power becomes 2 which corresponds to the Lorentzian shape of the spin resonance. For small interaction g_0 between fermions, $K_c \simeq 1 - g_0/\pi$, $v_s = v_F$, and $v_c \simeq v_F(1+g_0/\pi)$, so that the power deviates from 2 by $\sim (\delta v)^2 g_0^2$. Therefore, in the framework of perturbation theory the shape of the resonance line near $\omega_{\rm res}$ deviates slightly from Lorentzian. However, generally $g_0 = (e^2/\kappa\hbar v_F)|\ln qa|$ can be of the order of 1. For repulsive interactions $0 < K_c < 1$ and for strong fermionic interaction $K_c \to 0$. In this case the results (42) and (43) show that the shape of the absorption line may deviate significantly from Lorentzian at sufficiently strong interaction.

4. Spin fluctuations in a QW

In previous sections it was shown that the SOI resonance shoud exist at low enough temperature. However its observation by the measurement of the ac electromgnetic field adsorption is difficult since the signal is too weak to be resolved unless the sourse has the highest power achievable with modern technique. In addition the sample must be maintained at helium temperature. Therefore we propose instead to measure the total spin fluctuation in real time employing the experimental technique developed by S.A. Crooker and his team at LANL [17]. In their method the fluctuating spin produces the rotation of the polarization of light. The measurement of the polarization angle are rather sensitive. Therefore, the instant value of spin can be measured with high precision. In this method there is no need in the powerful incident electromagnetic wave. Instead a weak polarization rotation gives necessary information. In the original experiments they studied fluctuations of the spin in a quantum dot. The number of electrons in such a dot is comparable with that in the quantum wire. So far the time resolution was in the range about 0.1 ns that corresponds to the frequency 10 GHz. An experimental group in Germany has developed ultrafast spin spectroscopy and achieved frequency resolution up to hundreds GHz [56]. The SOI resonance will give a singularity in the spin fluctuation correlator in this range of frequency.

But the measurement of the spin correlator of the QW in this range of frequency at helium temperature can give also another very interesting information on the state of electron system. As we mentioned earlier, Starykh and coworkers [18] have found theoretically that at large enough external magnetic field perpendicular to internal one the QW develops a static spin-density wave (SDW) structure with the wave vector $2k_F$, an inhomogeneous state with physical properties rather different from those of the LL. So far this prediction was not checked experimentally.

In the bulk static magnetic structures with zero total spin can be found by applying slow neutron diffraction. In the QW the neutron scattering is too weak and the neutron diffraction cannot be applied. But spin correlation method is ideal to distinguish two alternative states of the QW: LL and SDW.

In this section we calculate spin correlators in the 1D interacting electron system with the SOI for both the ordinary LL and the SDW states.

4.1. Model

We use the same model of the LL with the SOI of the Rashba–Dresselhaus type as in previous section. However, some limitation will be imposed on the parameters. Besides of that in this section we study the action of external

magnetic field that has both parallel and perpendicular components. Therefore we start this subsection again with the definition of the model and its Hamiltonian.

We assume zero temperature and the length l of the QW to be much larger than any other scale of length. We remind that the most general SOI Hamiltonian has the form

$$H_{SOI} = \alpha(\hat{n}\cdot\boldsymbol{\sigma})p. \qquad (44)$$

The SOI coupling constant α has dimensionality of velocity. We assume it to be small: $\alpha << v_F$. Further in this section we put $\hbar = 1$ and apply everywhere wave vector k instead of momentum p. We denote the direction of internal field as z axis in the spin space and assume that the external field lies in the $x-z$ plane. Then the total Hamiltonian of electrons reads

$$H = \sum_i [\frac{k_i^2}{2m} + (\alpha k_i - b_{\|})\sigma_{i,z} - b_{\perp}\sigma_{i,x}] + H_{\text{int}}, \qquad (45)$$

where i labels electrons; H_{int} denotes the Hamiltonian of the electron-electron interaction and $b = g\mu_B B$. We assume external field to be weak: $b << \alpha k_F$.

The time-ordered spin correlators are defined as

$$S^T_{aa}(t) = \langle T_t S_a(t) S_a(0)\rangle = \langle e^{iH|t|} S_a e^{-iH|t|} S_a\rangle, \qquad (46)$$

where $S_a(t)$ is the total spin projection operator along direction $a = x, y, z$, and $\langle\rangle$ denotes the average over the ground state. The retarded correlators can be obtained from the time-ordered ones as $S^R_{aa}(t) = -2\theta(t)\text{Im}\, S^T_{aa}(t)$ [15], where $\theta(t)$ is the Heaviside step function.

In the absence of the SOI interaction the Hamiltonian of interacting electron system is invariant with respect to the group $SU(2)$ of rotations in the spin space. In the presence of the SOI interaction (finite value of α) and/or finite parallel field $b_{\|}$ the symmetry is reduced to the group $U(1)$ of rotations around direction of the internal field. In the presence of perpendicular field $b_{\perp}$ the $U(1)$ symmetry is also broken.

4.2. Ideal 1d Fermi gas

Before calculating the spin correlators of interacting electrons, it is instructive to solve the same problem for the ideal 1D Fermi gas. In the presence of the SOI and the external magnetic field, the spectrum consists of a pair of asymmetric parabola with avoided crossing as shown in Fig. 3. If $b << \alpha k_F$ and $\alpha << v_F$, the four Fermi momenta are approximately

$$k_{\sigma\tau} = \tau k_F - \sigma m\left[\alpha - \tau\frac{b_{\|}}{k_F} + \frac{b_{\perp}^2}{2k_F(\alpha k_F - \tau b_{\|})}\right],$$

where $\sigma = \pm$ denotes the spin-up/down bands and $\tau = \pm$ denotes right/left movers. At $T = 0$ spin correlators can be obtained directly by calculating the ground state average. The results at $b = 0$ read

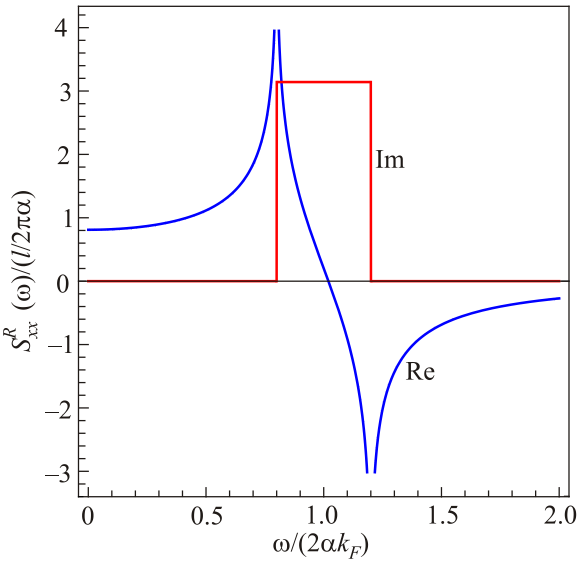

Fig. 3. (Color online). Total spin correlators for ideal 1D Fermi gas (Eq. (48)). $S^R_{xx}(\omega)$, both its real (blue) and imaginary (red) parts, are shown in unit $l/(2\pi\alpha)$ as functions of $\omega/(2\alpha k_F)$ at $m\alpha/k_F = 0.2$. Note that $S^R_{yy}(\omega) = S^R_{xx}(\omega)$, and $S^R_{zz}(\omega)$ vanishes.

$$S^R_{xx}(t) = S^R_{yy}(t) = \theta(t)\frac{2l}{\pi\alpha t}\sin(2\alpha k_F t)\sin(2m\alpha^2 t),$$
$$S^R_{zz}(t) = 0, \qquad (47)$$

where l is the wire's length, and spins are in units $\hbar/2 \equiv 1/2$. The Fourier transforms are

$$S^R_{xx}(\omega) = S^R_{yy}(\omega) = \frac{l}{2\pi\alpha}\log\frac{(\omega+i\delta)^2 - [2\alpha(k_F + m\alpha)]^2}{(\omega+i\delta)^2 - [2\alpha(k_F - m\alpha)]^2},$$
$$S^R_{zz}(\omega) = 0, \qquad (48)$$

where $\delta = 0^+$. The x and y components are equal and the z component vanishes, respecting the $U(1)$ symmetry. The imaginary part of $S^R_{xx}(\omega)$ has a narrow peak around $\omega = 2\alpha k_F$ of the width $4m\alpha^2$. In the resonance interval of frequency $2\alpha(k_F - m\alpha) < |\omega| < 2\alpha(k_F + m\alpha)$, the absorption intensity $\text{Im}\, S^R_{xx}$ is constant, as is seen in Fig. 3. Disorder can change this exotic shape of line.

4.3. Interacting electrons and bosonization

For interacting electrons we apply the LL theory described in the previous section. As it was discussed earlier, in 1D the interaction between fermions near Fermi points is always strong enough to make the collective Bose excitations almost independent instead of fermionic excitations in the Landau–Fermi liquid. Before translation to the bosonic language (bosonization), the original quadratic spectrum of fermions is linearized around the Fermi points, and the infinite sea of negative energy levels is filled. The extension of the fermion spectrum to $-\infty$ contrasts with the

initial spectrum of fermions limited from below. It does not lead to mistakes in physical results if the substantial range of momenta is close to the Fermi points. However in some problems a broader range of momentum is important. Namely this happens in the case of the total spin correlators as it will be shown in this subsection. In this situation the LL theory can be used only together with a proper cut-off of negative momenta. In this section we introduce an extension of the LL model to take in account more explicitly the interaction of electrons at opposite Fermi points. Thus, the interaction Hamiltonian in the model has the following form:

$$H_{\rm int} = \frac{1}{2}\sum_{\sigma,\sigma'}\int dxdx' U(x-x')\Psi^{\dagger}_{\sigma}(x)\Psi^{\dagger}_{\sigma'}(x')\Psi_{\sigma'}(x')\Psi_{\sigma}(x). \tag{49}$$

The interaction potential $U(x-x')$ will not be specified apart of its repulsive short-ranged character. The Fermi-field operator is the sum of the fields related to right and left movers:

$$\Psi_{\sigma}(x,t) = \sum_{\tau=\pm 1}\Phi_{\sigma,\tau}(x,t)e^{ik_{\sigma,\tau}x}, \tag{50}$$

where $k_{\sigma,\tau}$ are the four Fermi points for electrons with the spin projection σ, whereas $\tau = \pm 1$ label right and left movers. After the bosonization described in some details in the Appendix E, the resulting Hamiltonian is expressed in terms of the charge fields φ_c and θ_c and spin fields φ_s and θ_s. It differs from the Hamiltonian (34) of the Sec. 3 by the important term H_C responsible for the formation of the SDW (it was omitted in Sec. 3 since it is irrelevant in the LL state):

$$H_C = \frac{g_C}{2(\pi a_0^2)}\int \cos\left(\sqrt{8\pi}\varphi_s - \frac{4b_{\|}}{v_F}x\right)dx. \tag{51}$$

The connection between the Luttinger constants K_c, K_s and Fourier components $\tilde{U}(q)$ of the interaction potential are [15,16]

$$K_c = \left\{1+\left[2\tilde{U}(0)-\tilde{U}(2k_F)\right]/(\pi v_F)\right\}^{-1/2}, \tag{52}$$

$$K_s = \left\{1-\tilde{U}(2k_F/(\pi v_F)\right\}^{-1/2}. \tag{53}$$

The velocities of the charge and spin waves are $v_c = v_F/K_c$ and $v_s = v_F/K_s$, respectively. We neglected a correction $\alpha b_{\|}/v_F << k_f$ in the argument of $\tilde{U}$ and ignored a term mixing charge and spin fields that has the relative order of magnitude $\sim \alpha/v_F << 1$. The charge and spin degrees of freedom in this Hamiltonian are separated. The charge Hamiltonian is quadratic, but the spin Hamiltonian contains a cosine backscattering term H_C. If the latter can be neglected, the remaining quadratic Hamiltonian H_s describes the ordinary LL state. When H_C dominates, the field φ_s becomes pinned to one of the minima of cosine, resulting in ordering in the spin sector of the SDW state.

4.4. SDW in weak magnetic field

Starykh *et al.* [18] proved that static SDW appears when the external field is directed perpendicular to the internal one and strongly exceeds it. We consider a more realistic limit $b << \alpha k_F$, and first fix $b_{\perp} = 0$. The charge Hamiltonian H_c is quadratic and does not change in the magnetic field. To renormalize the spin part, we define following [18] spin currents:

$$J^i_{\tau} = \Phi^{\dagger}_{\tau}\sigma_i\Phi_{\tau}, \tag{54}$$

where σ_i $(i = x, y, z)$ are three Pauli matrices. The two-component spinors Φ_{τ}, with $\tau = R, L$ corresponding to the left and right movers, are defined by Eq. (50). The spin part of the Hamiltonian H_s can be expressed in terms of these currents as follows:

$$H_s = 2\pi v_s'\int dx\left\{\sum_{\tau}(J^z_{\tau})^2 + y_s J^z_R J^z_L + \right.$$
$$+ y_C\left[\cos\frac{4b_{\|}x}{v_F}\left(J^x_R J^x_L + J^y_R J^y_L\right) + \right.$$
$$\left.\left. + \sin\frac{4b_{\|}x}{v_F}\left(J^x_R J^x_L - J^y_R J^y_L\right)\right]\right\}, \tag{55}$$

where $v_s' = \sqrt{2v_s^2(0) - v_f^2} = v_F[1-\tilde{U}(2k_F)/(2\pi v_F)]$. The initial values of coupling constants are $y_s(0) = y_c(0) = -\tilde{U}(2k_F)/(\pi v_s')$. The contants y_s, y_C are connected to the constants K_s and g_C by relations $K_s = \sqrt{(2-y_s)/(2+y_s)}$, $g_C = -\pi v_s' y_C$.

At $b_{\|} = 0$, the Hamiltonian H_s becomes simplifies to the following form:

$$H_{s0} = 2\pi v_s'\int dx\left\{\sum_{\tau}\left(J^z_{\tau}\right)^2 + y_s J^z_R J^z_L + \right.$$
$$\left. + y_C\left(J^x_R J^x_L + J^y_R J^y_L\right)\right\}. \tag{56}$$

The renormalization group equations for this Hamiltonian in the one-loop approximation are

$$\frac{dy_s}{d\lambda} = y_C^2; \quad \frac{dy_C}{d\lambda} = y_s y_C. \tag{57}$$

Here λ is the standard renormalization group running parameter (logarithm of the length scale l). The renormalzation group equations have a simple integral of motion $y_C^2 - y_s^2 = \text{const}$. Since it is zero at initial scale $l = a_0$, it remains zero at any length scale. The point $y_s = y_C = 0$ is the fixed point of the system (57), whereas the pair of the straight lines in the plane y_s, y_C defined by equation $y_s^2 = y_C^2$ is the separatrix of the trajectories that are generally hyperboles. The motion along separatrix at increasing λ leads to the fixed

point. Since both charges y_s and y_C are zero in the fixed point, according to the relations written above we find that at large length scale $g_C \to 0$ and $K_s \to 1$. Thus, at zero magnetic field the cosine interaction is irrelevant. The limiting value of K_s shows that the $SU(2)$ symmetry violated at small distance is restored on large distances. The system remains in the LL state.

The same answer is correct in the presence of the parallel magnetic field since the oscillations associated with rotation of spin around this field stops renormalization at the scale $l_{\|} = v_F / b_{\|}$. However, if $b_{\|} = 0$ but $b_{\perp} \neq 0$, the situation changes. More complicated analysis shows that in this case renormalization leads to $y_s = Y_C = -\infty$ at $\lambda \to \infty$. Though, this result can be treated as the requirement of very precise orientation of the external field for observation of the SDW, this limitation is much more liberal for real QW because of their finite length. Indeed the field must be perpendicular if the length of wire is much larger than $l_{\|}$, or $b_{\|} << v_F / l$. For the length 10 μm it requires parallel magnetic field less than 0.6 T.

4.5. Spin-density correlations

In this subsection we calculate the spin-density correlators for the ordinary LL state and the SDW state. At $b << \alpha k_F$, the Fermi momenta are approximately $k_{\sigma,\tau} = \tau k_F - \sigma m\alpha$. In the ordinary LL state, the backscattering term HC can be dropped and the Hamiltonian becomes completely quadratic. The Luttinger parameters are given in the previous subsection, except of $K_s = 1$ at zero external field. Spin density operators read: $s_a(x) = \Psi^{\dagger}_{\sigma}(x)\sigma_{a,\sigma\sigma'}\Psi_{\sigma'}(x)$, where $a = x, y, z$. The time-ordered spin-density correlators are $s_{aa}(x,t) = \langle T_t s_a(x,t) s_a(0,0)\rangle$. Applying the bosonization one can express spin correlators as path integrals over bosonic fields. Details of calculation are placed in Appendix F. The results are

$$s_{xx}(x,\tau) = s_{yy}(x,\tau) = \frac{a_0^{K_s+\frac{1}{K_s}-2}}{\pi^2}\frac{(y_s^2 - x^2)\cos(2m\alpha x)}{(x^2+y_s^2)^{1+\frac{K_s}{2}+\frac{1}{2K_s}}} +$$

$$+\frac{a_0^{K_c+\frac{1}{K_s}-2}}{\pi^2}\frac{\cos(2k_F x)\cos(2m\alpha x)}{(x^2+y_c^2)^{K_c/2}(x^2+y_s^2)^{1/2K_s}},$$

$$s_{zz}(x,\tau) = \frac{K_s}{\pi^2}\frac{y_s^2 - x^2}{(x^2+y_s^2)^2} +$$

$$+\frac{a_0^{K_c+K_s-2}}{\pi^2}\frac{\cos(2k_F x)}{(x^2+y_c^2)^{K_c/2}(x^2+y_s^2)^{K_s/2}}, \qquad (58)$$

where $y_{s/c}(\tau) = v_{s/c}\tau$, τ is imaginary time, and a_0 is an ultraviolet cut-off. Each correlator contains contributions from small q and from $q \sim 2k_F$. For weakly interacting case $K_c, K_s \approx 1$, and both decay as x^{-2} and oscillate.

The SDW state exists at completely perpendicular field, when y_C flows to the strong coupling limit $y_C \to -\infty$. H_C is relevant and dominates the spin Hamiltonian. The field φ_s is pinned to $\varphi_s = (N + \frac{1}{2})\sqrt{\frac{\pi}{2}}$ (N is an integer), whereas its conjugated field θ_s is completely uncertain. Correlators of the charge fields remain the same as in ordinary LL. The correlators $s_{xx}(x,\tau)$ and $s_{yy}(x,\tau)$ decay exponentially to zero being averaged with the oscillating factor $e^{i\theta_s}$. But $s_{zz}(x,\tau)$ survives since θ_s doesn't appear in its expression:

$$s_{zz}(x,\tau) = \frac{2}{(\pi a_0)^2}\cos(2k_F x)\left(\frac{a_0}{\sqrt{x^2+y_c^2}}\right)^{K_c}. \qquad (59)$$

It is determined exclusively by the charge degrees of freedom. It oscillates with the wave vector $2k_F$ and decays power-like with $\sqrt{x^2+y_c^2}$. For $K_c \approx 1$ it decays as x^{-1} which is slower than x^{-2} decay of the ordinary LL case. This is the result of ordering in the SDW state.

4.6. Total spin correlations

The total spin correlator can be obtained by integration of spin-density correlators found in previous subsection over coordinates. Eqs. (58) and (59) present the time-ordered spin-density correlators for imaginary time τ. Let define the total spin-correlation function with imaginary time interval

$$S^T_{aa}(\tau) = \int_0^l\int_0^l dx\,dx' s_{aa}(x-x',\tau) \approx l\int_{-\infty}^{\infty} s_{aa}(x,\tau)$$

and their Fourier transforms

$$S^T_{aa}(\omega) = \int_{-\infty}^{\infty} e^{i\omega\tau} S^T_{aa}(\tau).$$

The Fourier transform of the retarded correlator $S^R_{aa}(t)$ is the analytic continuation of the time-ordered Fourier transform $S^R_{aa}(\omega) = S^T_{aa}(i\omega \to \omega + i\delta)$, where $\delta = 0^+$ [15]. For details of calculation see Appendix G.

In this point we are faced with a paradox: the integrated over x correlator $s_{zz}(x,\tau)$ in the absence of the transverse external magnetic field is not a constant in contradiction with the exact conservation of the z component of the total spin. For the SDW state $S^R_{zz}(\omega)$ is also not a constant, but the SDW appears only in nonzero transverse field that violates the S_z conservation. Such a contradiction was first noted by Tennant *et al.* [57] (see their appendix) and they

treated it phenomenologically assuming that the oscillating term is a complete derivative. This discrepancy originates in the filling of infinite Fermi sea, a crucial assumption in the LL model [15,16]. Electron and hole excitations in this model are completely symmetric. In real wires the relativistic particle-hole symmetry is violated. In particular, the momenta of holes cannot exceed k_F by modulus. This limitation is not important if only momenta close to $\pm k_F$ are essential. This is the case for the spin-Peierls instability leading to the appearance of the SDW. However, the momenta far from k_F bring a significant contribution to the total spin. Therefore, the LL model does not respect the total spin conservation. Nevertheless, calculations for the non-interacting case within the Fermi gas model shows that the cut-off of the integration at some negative momentum k_D leads to conserving S_z if $k_D < k_F$. This cut-off produces additional terms in the spin-density correlator so that at $k_D = 0$,

$$s_{zz}(x,\tau) = \frac{1}{\pi^2}\frac{y^2-x^2}{(x^2+y^2)^2} + \frac{1}{\pi^2}\frac{\cos(2k_F x)}{x^2+y^2} - \\ -\frac{2}{\pi^2}\frac{y(y\cos(k_F x) - x\sin(k_F x))\mathrm{e}^{-k_F y}}{(x^2+y^2)^2}, \qquad (60)$$

where $y = v_F\tau$. The third term in Eq. (60) is the cut-off correction. After integration over x it completely cancels the contribution of the second term. The first term is contribution of small momentum transfer. Its integration gives zero. Though it is not clear how to introduce the momentum cut-off for interacting electrons, the main conclusion that we can extract from the calculations for free electrons is that the momentum transfer $2k_F$ does not contribute anything to the zz correlation of the total spins at $B_\perp = 0$. Further we leave only small momentum contribution to this correlator. We then arrive at a simple result for the LL state:

$$S^R_{xx}(\omega) = S^R_{yy}(\omega) = A_0[\omega_s^2 + (\omega+i\delta)^2]\times \\ \times[\omega_s^2 - (\omega+i\delta)^2]^{\frac{K_s}{2}+\frac{1}{2K_s}-2}, \quad S^R_{zz}(\omega) = 0. \qquad (61)$$

where $\omega_s = 2m\alpha v_s$ and

$$A_0 = \frac{l(\frac{a_0}{2v_s})^{K_s+\frac{1}{K_s}-2}\Gamma(2-\frac{K_s}{2}-\frac{1}{2K_s})}{\pi v_s\Gamma(1+\frac{K_s}{2}+\frac{1}{2K_s})}.$$

The SDW state that appears only in the transverse field violating the total spin conservation does not require such a fine tuning. Its total spin correlators are

$$S^R_{xx}(\omega) = S^R_{yy}(\omega) = 0, \\ S^R_{zz}(\omega) = A_{SDW}[\omega_{0c}^2 - (\omega+i\delta)^2]^{\frac{K_c}{2}-1}, \qquad (62)$$

where $\omega_{0c} = 2k_F v_c$, and

$$A_{SDW} = \frac{2l(\frac{a_0}{2v_c})^{K_c-2}\Gamma(1-\frac{K_c}{2})}{\pi v_c\Gamma(\frac{K_c}{2})}.$$

We summarize the major differences between these two states in Table 1. The line shapes of the non-vanishing spin correlators for both states are shown in Figs. 4 and 5.

Table 1. Major differences of the total spin correlations between the LL and SDW states

State	Vanishing component	Position of singularity for nonvanishing component
LL	S_{zz}	$\omega = 2m\alpha v_s \approx 2k_F\alpha$
SDW	S_{xx}, S_{yy}	$\omega = 2k_F v_c$

4.7. Relation to the experiment

The results given by Eqs. (61) and (62) show that measurements of the total spin correlators can be used as a diagnostic tool for identification of the state of the electronic liquid in the quantum wire, is it the LL or the SDW. Besides of that we predict that in the ordinary LL state the transverse correlators display the spin resonance at $\omega_s = 2m\alpha v_s \approx 2k_F\alpha$.

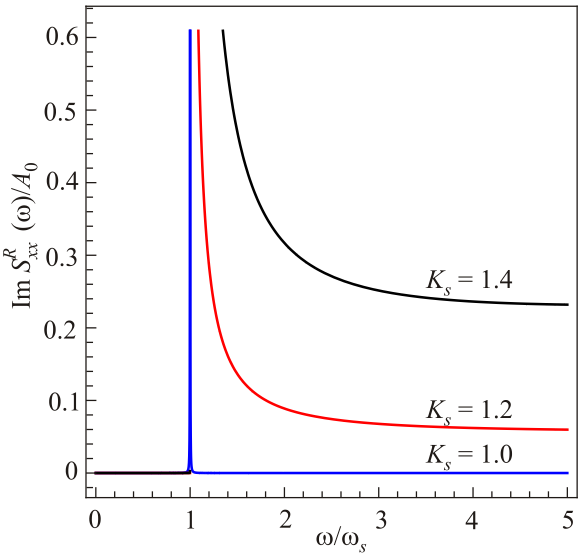

Fig. 4. (Color online). Total spin correlators for the LL state (Eq. (61)). $\mathrm{Im}\, S^R_{xx}(\omega)$ is shown in unit A_0 as a function of ω/ω_s for $K_s = 1$ (blue), 1.2 (red) and 1.4 (black). The $K_s = 1$ curve is a δ-function spike at $\omega = \omega_s$. $S^R_{zz}(\omega)$ vanishes for the LL state.

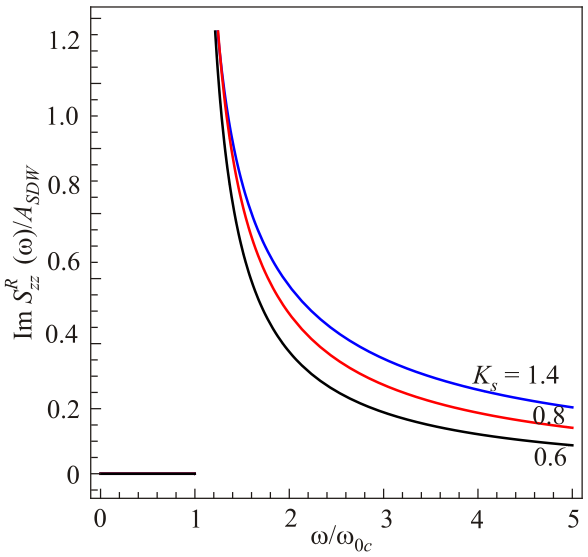

Fig. 5. (Color online). Total spin correlators for the SDW state (Eq. (62)). Im $S^R_{zz}(\omega)$ is shown in unit A_{SDW} as a function of ω/ω_{0c} for $K_c = 1$ (blue), 0.8 (red) and 0.6 (black). $S^R_{xx}(\omega)$ and $S^R_{yy}(\omega)$ vanish for the SDW state. Note that if $\alpha << v_F$ and $v_s \approx v_c \approx v_F$, we have $\omega_{0c} >> \omega_s$.

The position of resonance agrees with the previous non-interacting result (48). In the SDW state only the z correlator survives and it has a peak at a relatively high $\omega_{0c} = 2k_F v_c \approx 2k_F v_F$. A typical value for this frequency in semiconductors is 10^{14} Hz. At much lower frequency it is almost constant.

Experimentally, the Faraday rotation method [17,55] measures directly the spin correlations in real time. At zero field the system is in the ordinary LL state, and we expect peaks at $\omega = 2m\alpha v_s$ for directions perpendicular to the SOI axis. The direction of the SOI axis is not a priori known. It must be found utilizing the $U(1)$ symmetry of the transverse spin correlations. Applying the magnetic field perpendicular to the SOI axis, one can check whether the wire transits to the SDW state. At this transition the longitudinal correlator suppressed in the LL state becomes dominant, whereas the transverse correlators are suppressed.

The impurity scattering does not change the results significantly if the mean free path is larger than $1/(m\alpha)$, typically 10–30 nm. The corresponding mobility is $\sim(1–3)\cdot10^3$ cm^2/(V·s).

5. Conclusions

Our theory is based on conservation of the total spin in 1d quantum electron system subject to the SOI. The effective SOI field acting on electron spins has a definite direction tilted to the direction of the wire. Projection of the total spin on this direction is conserved. Theory predicts the existence of the SOI-induced spin resonance in semiconductors at low temperature $T < 4m\alpha^2 \sim 3$ K. The resonance can be regulated by external magnetic field. Its component perpendicular to the internal field switches on the electric dipolar mechanism of the spin-flip transition and strongly enhances the probability of the resonance absorption. The component of the external field parallel to the internal one may separate resonances for the left and right movers. In this way the permanent electric current can be generated by the resonance ac electromagnetic field. These phenomena obtained first in the model of ideal elctron gas are confirmed in a more realistic model of LL for electrons. In the framework of this model the resonance excites a spinon, an excitation of the spin component of the LL with the wave vector equal to the difference between Fermi momenta of the left and right movers due to the SOI splitting. An additional effect is the spin-flip process induced by a plasmon excitation due to a weak coupling between spin and charge degrees of freedom generated by the SOI.

Experimentally the SOI-induced spin resonance manifests itself most directly in the resonance absorption of electromagnetic field with frequency about 1 THz. Such an experiment requires large power of the ac field (1 kW/cm^2) so far available only with free elecron laser. Additional requirements of He temperature and magnetic fields in the range of several Tesla makes this experiment difficult.

An alternative idea is to diagnose the LL state in a semiconductor (InGaAs) by measurements of the total spin correlation in real time proposed by Crooker at ANL [17]. These measurements are less direct. Their preference apart of a weak probe light field is that they can distinguish between the LL state and the SDW state of electron liquid in the wire predicted by Starykh and his coworkers at sufficiently strong perpendicular component of external field. So far this state was not observed experimentally. Our analysis of the total spin correlations shows that the SDW supresses fluctuations of the perpendicular to the inner field magnetization in the wire leaving only parallel components, whereas in the LL state perpendicular fluctuations are dominant, whereas the parallel component is suppressed. We hope that this effect can be used for diagnostic of the state of electrons in the quantum wire.

Acknowledgments

I am indebted to the coauthors of publications on which this review is based Artem Abanov, Wayne Saslow, Peng Zhu, Oleg Tretyakov, Konstantin Tikhonov and Chen Sun. My thanks are due to A. Finkelstein, L. Glazman, M. Khodas, J. Kono, O. Starykh and A. Tsvelik for enlightening discussions. My special thanks is to Chen Sun for his invaluable help in the preparation of the manuscript.

Appendix A. Spin-flip in a QW of a finite thickness

In this appendix we present the calculation referred to Sec. 2 of the matrix element responsible for the spin flipping due to coupling to the transverse electric field. We treat the spin-orbit interaction as a perturbation and show

that the matrix element is zero in the first and second order of the SOI coupling constants α and β. The first nonzero contribution comes in the third order in spin-orbit interaction. We start from the same Hamiltonian (1). We introduce the frame of reference with the x axis along the wire, y axis along the wide side of the cross-section whose linear size is denoted as W. Because we are only interested in the linear coupling to the y component of the electric field, we take A_x, A_z and the magnetic field B to be zero. Then the Hamiltonian, up to linear terms in the ac field, reads

$$H = H_{\rm kin} + H_{so} + H_{ac} \tag{63}$$

where

$$H_{\rm kin} = \frac{p_x^2 + p_y^2}{2m^*}, \tag{64}$$

$$H_{so} = p_x(\alpha\sigma_x + \beta\sigma_y) - p_y(\alpha\sigma_y + \beta\sigma_x), \tag{65}$$

$$H_{ac} = \frac{e}{c} A_y \upsilon_y. \tag{66}$$

Here $\upsilon_y = \dfrac{p_y}{m^*} - (\beta\sigma_x + \alpha\sigma_y)$ and we assume that the effective mass m^* is the same in both x and y directions. Let us represent the Hamiltonian (63) without the last term as $H = H_0 + V$, where $H_0 = H_{\rm kin} + p_x(\alpha\sigma_x + \beta\sigma_y)$ and the perturbation is $V = -p_y(\alpha\sigma_y + \beta\sigma_x)$. The stationary states $\left|n, p_x, \tau\right\rangle_0$ of the Hamiltonian H_0 are direct products of the eigenstates of p_x, p_y^2 and the spin operator $\tau_z = (\alpha\sigma_x + \beta\sigma_y)/\gamma$. The corresponding wave functions are

$$\psi^{(0)}_{n,p_x,\tau} = f_n(y) \mathrm{e}^{ip_x x} \chi_\tau \tag{67}$$

Here $f_n(y)$ is the transverse part of the wave function, and χ_τ is an eigenspinor of τ_z with the eigenvalue $\tau = \pm 1$. The energy of the state $\left|n, p_x, \tau\right\rangle_0$ is $E^0_{n,p_x,\tau} = E^0_{n,p_x} + \gamma p_F$, where $E^0_{n,p_x} = {}_0\langle n, p_x, \tau \left| H_{\rm kin} \right| n, p_x, \tau\rangle_0$. The first-order perturbation theory correction to the wave function (67) is

$$\psi^{(1)}_{n,p_x,\tau} = -\sum_{m\neq n,\tau'} \left|m, p_x, \tau'\right\rangle_0 \times$$

$$\times \frac{{}_0\langle m, p_x, \tau' \left| (\alpha\sigma_y + \beta\sigma_x) p_y \right| n, p_x, \tau\rangle_0}{E^0_{n,p_x} - E^0_{m,p_x}}, \tag{68}$$

where we neglect the contribution of the first SOI term $p_x(\alpha\sigma_x + \beta\sigma_y)$ to the energies in denominator retaining the leading term $E^0_{n,p_x} - E^0_{m,p_x}$. In order to calculate the sum in Eq. (68) we note that $p_y = \dfrac{im^*}{\hbar}[H_{\rm kin}, y]$. Then this equation can be simplified as follows:

$$\psi^{(1)}_{n,p_x,\tau} = \frac{im^*}{\hbar} \sum_{m\neq n,\tau'} \left|m, p_x, \tau'\right\rangle_0 \times$$

$$\times {}_0\langle m, p_x, \tau' \left| (\alpha\sigma_y + \beta\sigma_x) y \right| n, p_x, \tau\rangle_0. \tag{69}$$

Finally by choosing the frame of coordinates so that $\langle n \left| y \right| n\rangle = 0$ and using the completeness relation $\sum_{m,\tau'} \left|m, p_x, \tau'\right\rangle_0 {}_0\langle m, p_x, \tau' \right| = I$, we find the first order correction to the eigenstate $\left|n, p_x, \tau\right\rangle_0$

$$\left|n, p_x, \tau\right\rangle_1 = \frac{im^*}{\hbar} (\alpha\sigma_y + \beta\sigma_x) y \left|n, p_x, \tau\right\rangle_0. \tag{70}$$

Now we consider the effect of the transverse ac electric field. We are interested in the off-diagonal term of the operator $\dfrac{e}{c} A_y \upsilon_y$ for the states of a fixed band, i.e., in the matrix element

$$\frac{e}{c} A_y \langle n, p_x, - \left| \upsilon_y \right| n, p_x, +\rangle, \tag{71}$$

where + and − represent the up and down eigenstates of the spin operator τ_z, respectively. Again employing the Heisenberg equation $\upsilon_y = \dfrac{i}{\hbar}[H_{\rm kin} + H_{so}, y]$, one can transform the matrix element (71) as follows:

$$\langle n, p_x, - \left| \upsilon_y \right| n, p_x, +\rangle =$$

$$= \frac{i}{\hbar} (E_{n,p_x,-} - E_{n,p_x,+}) \langle n, p_x, - \left| y \right| n, p_x, +\rangle. \tag{72}$$

The energies belonging to a fixed band n and different spin projections differ only because of the SOI. Therefore, an expansion of the difference $E_{n,p_x,-} - E_{n,p_x,+}$ in terms of SOI coupling constants begins with a linear term of α and β:

$$E_{n,p_x,-} - E_{n,p_x,+} \approx -2\gamma p_x. \tag{73}$$

Thus, to obtain the contribution to the matrix element (72) linear in SOI coupling constants, it is necessary to calculate the matrix element of y with the zeroth-order wave function $\left|n, p_x, \tau\right\rangle_0$ $(\tau = \pm 1)$ for which the space and spin variables are factored. Therefore, the matrix element of y contains the scalar product $\langle - \left| + \right\rangle$, which equals zero. To find the matrix element in Eq. (72) to second order in α and β, we need to use $\left|n, p_x, \tau\right\rangle_1$ for the matrix element of y. Then, using Eq. (70), one finds

$${}_1\langle n, p_x, - \left| y \right| n, p_x, +\rangle_0 + {}_0\langle n, p_x, - \left| y \right| n, p_x, +\rangle_1 =$$

$$= \frac{im^*}{\hbar} {}_0\langle n, p_x, - \left| (\alpha\sigma_y + \beta\sigma_x)[y, y] \right| n, p_x, +\rangle_0. \tag{74}$$

Since this matrix element is zero, the y component of the electric field produces no spin-flip processes in the second order in α and β as well.

The quickest way to calculate the Hamiltonian H_{ac} in the third order or, equivalently, the matrix element of y in the second order goes through a unitary transformation $U = \mathrm{e}^F$, where $F = -i\dfrac{m^*}{\hbar} y(\alpha\sigma_y + \beta\sigma_x)$. Applying it to the Hamiltonian (without the ac field term), and truncating the Baker–Hausdorff series at the second order of α and β (recall that $\gamma = \sqrt{\alpha^2 + \beta^2}$), we find

$$H_U = U(H_{\rm kin} + H_{so})U^{-1} \approx H + [F, H] = \\ = H_0 + V_U + \text{const}, \tag{75}$$

where

$$H_0 = \frac{p_x^2 + p_y^2}{2m^*} + p_x\gamma\tau_z \tag{76}$$

is the starting approximation Hamiltonian introduced earlier and

$$V_U = \frac{2m^*}{\hbar}(\beta^2 - \alpha^2) y p_x \sigma_z \tag{77}$$

is the transformed perturbation that is proportional to squares of the SOI constants. Note that the transformed eigenstate $\left|n, p_x, \tau\right\rangle_U$ obeys the same boundary conditions as the initial one. Thus, the transformed state $\left|n, p_x, \tau\right\rangle_U$ differs from zero approximation state $\left|n, p_x, \tau\right\rangle_0$ by the second order correction

$$\left|n, p_x, \tau\right\rangle_{U,2} = \frac{2m^* p_x}{\hbar}(\beta^2 - \alpha^2) \sum_{m\neq n,\tau'} \left|m, p_x, \tau'\right\rangle_0 \times \\ \times \frac{{}_0\left\langle m, p_x, \tau' \right| y\sigma_z \left| n, p_x, \tau\right\rangle_0}{E^0_{n,p_x} - E^0_{m,p_x}}. \tag{78}$$

The state vector we are looking for $\left|n, p_x, \tau\right\rangle = U^{-1}\left|n, p_x, \tau\right\rangle_U$ has an additional term of the second order equal to the operator $F^2/2$ acting on the zeroth order state. Since F^2 is proportional to unit operator, it does not contribute to the matrix element in Eq. (72). With Eqs. (67), (72), (73), (78), we obtain the matrix element to the third order in α and β:

$$\left\langle n, p_x, -\right| \upsilon_y \left| n, p_x, +\right\rangle = -\sum_{m\neq n} \frac{i}{\hbar}\frac{8m^* p_x^2}{\hbar}\gamma(\beta^2 - \alpha^2) \times \\ \times \frac{\left|{}_0\left\langle m, p_x \right| y \left| n, p_x\right\rangle_0\right|^2}{E^0_{n,p_x} - E^0_{m,p_x}}, \tag{79}$$

where we use matrix elements for spin operator σ_z between the eigenstates of the operator τ_z $\left\langle \pm\right|\sigma_z\left|\pm\right\rangle = 0$ and $\left\langle \mp\right|\sigma_z\left|\pm\right\rangle = 1$. The zero order off-diagonal matrix element reads

$${}_0\left\langle m, p_x \right| y \left| n, p_x\right\rangle_0 = -\frac{8nmW\sin(\dfrac{m+n}{2}\pi)}{\pi^2(m^2 - n^2)^2}, \tag{80}$$

and

$$E^0_{n,p_x} - E^0_{m,p_x} = \frac{\hbar^2\pi^2(n^2 - m^2)}{2m^* W^2}. \tag{81}$$

Thus, the matrix element of the velocity υ_y from Eq. (72) can be expressed in terms of an infinite series:

$$\left\langle n, p_x, -\right| \upsilon_y \left| n, p_x, +\right\rangle = i(\beta^2 - \alpha^2)\gamma \frac{1024 m^{*2} W^4 p_x^2 n^2}{\hbar^4\pi^6} \times \\ \times \sum_{m=n+odd} \frac{m^2}{(m^2 - n^2)^5}. \tag{82}$$

For $n = 1$ the sum is

$$\sum_{k=1}^{\infty} \frac{4k^2}{(4k^2 - 1)^5} = \frac{\pi^2(15 - \pi^2)}{3072} \approx 0.01648.$$

We can now obtain the coefficient at $e/cA_y\upsilon_y$ for the spin-flip amplitude induced by the transverse electric field and it is given by

$$i\gamma \frac{m^{*2} W^4 p_x^2(\beta^2 - \alpha^2)}{\hbar^4} \cdot 0.0176. \tag{83}$$

If we let $W = 10$ nm, $p_F = 1.65\cdot 10^{-21}$ g·cm/s, $\alpha = 1.08\cdot 10^6$ cm/s and $v_F = 0.38\cdot 10^8$ cm/s, then we find that the upper bound for the coefficient at γ given by Eq. (83) is $\sim 10^{-5}\gamma$. It is by 5 decimal orders less than the coefficient (γ) of $(e/c)A_x\tau_z$. However, the latter does not produce a spin-flip transition. The transverse magnetic field makes spin-flips possible but decreases the coefficient by a factor $(b_\perp/\gamma p_F)^2 \sim 0.01$. Nevertheless the anisotropy ratio of the amplitudes is about 0.001. The anisotropy of the spin-flip probability is about 10^{-6}. Thus, resonant excitation by an ac electric field polarized along the y axis is very ineffective and practically unobservable. However, the amplitude (83) depends very strongly on W. Therefore, the width can not be increased significantly. On the other hand, a significant change of W would violate the condition of one channel.

Appendix B. Calculation of time-ordered averages in real time

To find the correlation functions of fields φ_s and θ_s in Eq. (35) we use the generating functional $\mathcal{Z}[\mathbf{J}]$:

$$\mathcal{Z} = \int \mathcal{D}\varphi_i \mathcal{D}\theta_i \exp\left[\int d\tau \int dx \left(-\frac{1}{2}\overline{\Phi} M \Phi + \overline{J}\Phi\right)\right]. \tag{84}$$

This expression is written in a matrix form with four vectors of the field $\overline{\Phi}=(\varphi_c,\varphi_s,\theta_c,\theta_s)$ and "current" $\overline{J}=(J_1,J_2,J_3,J_4)$. The 4×4 matrix M describes the system Lagrangian and is presented below. After the standard Gaussian integration we find

$$\mathcal{Z}[\mathbf{J}]=\left(\det M\right)^{-1/2}\exp\left(\frac{1}{2}\overline{J}M^{-1}J\right). \tag{85}$$

The bosonic correlation functions from Eq. (35) are represented in terms of the elements of matrix M as

$$\left\langle\Phi_i(x,\tau)\Phi_j(0,0)\right\rangle=\left.\frac{\delta^2\ln\mathcal{Z}}{\delta J_i(x,\tau)\delta J_j(0,0)}\right|_{\mathbf{J}=0}=$$

$$=\int\frac{d\omega}{2\pi}\int\frac{dq}{2\pi}e^{iqx-i\omega\tau}M^{-1}_{ij}(q,\omega). \tag{86}$$

The matrix M is symmetric and has the following nonzero elements

$$M_{\varphi_c\varphi_c}=v_cq^2/(\pi K_c),\quad M_{\varphi_s\varphi_s}=v_sq^2/(\pi K_s),$$

$$M_{\theta_c\theta_c}=v_cK_cq^2/\pi,\quad M_{\theta_s\theta_s}=v_sK_sq^2/\pi,$$

$$M_{\varphi_c\theta_c}=M_{\varphi_s\theta_s}=iq\omega/\pi,\text{ and}$$

$$M_{\varphi_c\theta_s}=M_{\varphi_s\theta_c}=\delta vq^2/(2\pi).$$

With these expressions, $g(x,t)$ in Eq. (35) takes the form

$$g(x,\tau)=2i\iint\frac{dqd\omega}{(2\pi)^2}(1-e^{iqx-i\omega\tau})[M^{-1}_{\varphi_s\varphi_s}(q,\omega)+$$

$$+M^{-1}_{\theta_s\theta_s}(q,\omega)-M^{-1}_{\varphi_s\theta_s}(q,\omega)-M^{-1}_{\theta_s\varphi_s}(q,\omega)]. \tag{87}$$

At zero SOI ($\alpha=0$) and magnetic field ($B_\perp=0$), the system has $SU(2)$ symmetry of spin rotation. This symmetry prevents the renormalization of the interaction constant in the spin channel and therefore $K_s=1$ [48]. A weak SOI ($\alpha\ll v_F$) and magnetic field ($B_\perp\ll\alpha p_F/\mu_B$) only slightly violate the $SU(2)$ symmetry [49], so that $K_s-1\sim(\alpha/v_F)^2$ [49]. Therefore, in what follows we put $K_s=1$ up to small corrections of order α^2. Thus, with this precision up to quadratic in δv terms we find

$$M^{-1}_{\varphi_s\varphi_s}(q,\omega)+M^{-1}_{\theta_s\theta_s}(q,\omega)-M^{-1}_{\varphi_s\theta_s}(q,\omega)-M^{-1}_{\theta_s\varphi_s}(q,\omega)\simeq$$

$$\simeq\frac{2\pi i}{q(\omega+iv_sq)}-(\delta v)^2\frac{\pi q}{4K_c}\frac{(K_c^2+1)v_cq+2iK_c\omega}{(\omega+iv_sq)^2(\omega^2+v_c^2q^2)}.$$

Performing the integration over frequencies, one finds the correlator as a function of imaginary time. Because of factor $e^{-i\omega\tau}$ only the poles in the lower half-plane of the complex plane ω contribute to the integral. After the integration and analytical continuation, expression (87) turns into a sum of logarithms of the type $C\ln(x\pm v_{c,s}t)$, where C is a constant. Inserting this result in Eq. (35) we find the corresponding time-ordered fermionic correlator but in real time.

Appendix C. Relation between retarded and time-ordered spin correlators

The perturbation theory is valid for time-ordered averages in imaginary time, whereas what we need to calculate is a retarded average $I^R_{\uparrow\downarrow,\downarrow\uparrow}(t)$. Therefore, we need a relationship between $I^R_{BA}(x,t)=-i\theta(t)\langle[B(x,t),A(0,0)]\rangle$ and $I^T_{BA}(x,\tau)=-\langle T_\tau B(x,\tau)A(0,0)\rangle$ for imaginary time τ where

$$B(x,t)=\psi^\dagger_{R,\uparrow}(x,t)\psi_{R,\downarrow}(x,t)$$

and

$$A(0,0)=\psi^\dagger_{R,\downarrow}(0,0)\psi_{R,\uparrow}(0,0)$$

are boson-like operators. These two types of averages are related by equality [15]

$$I^R_{BA}(t)=i\theta(t)\left[I^T_{BA}(t)-\left(I^T_{A^\dagger B^\dagger}(-t)\right)^*\right], \tag{88}$$

which follows from

$$I^R_{BA}(t)=-i\theta(t)\left[\left\langle B(t)A(0)\right\rangle-\left\langle A(0)B(t)\right\rangle\right], \tag{89}$$

$$I^T_{BA}(t)=-\left[\theta(t)\left\langle B(t)A(0)\right\rangle+\theta(-t)\left\langle A(0)B(t)\right\rangle\right]. \tag{90}$$

For positive time $t>0$,

$$I^T_{BA}=-\left\langle B(t)A(0)\right\rangle, \tag{91}$$

$$-\left(I^T_{A^\dagger B^\dagger}(-t)\right)^*=\left\langle B^\dagger(0)A^\dagger(-t)\right\rangle^*, \tag{92}$$

and

$$\left\langle B^\dagger(0)A^\dagger(-t)\right\rangle^*=\left\langle A(-t)B(0)\right\rangle=$$

$$=\left\langle A(0)B(t)\right\rangle=\left\langle B^\dagger(t)A^\dagger(0)\right\rangle^*.$$

In our case, due to the above definitions of A and B, $\left\langle B^\dagger(t)A^\dagger(0)\right\rangle$ differs from $\left\langle B(t)A(0)\right\rangle$ by changing the spin components $\sigma\to-\sigma$. It is equivalent to $Y(x,t)\to-Y(x,t)$ since we introduced $e^{Y(x,\tau)}/(2\pi a_0)=\psi^\dagger_{R\uparrow}(x,\tau)\psi_{R\downarrow}(x,\tau)$. However, Y enters in all correlation functions quadratically, see Eq. (35) in the main part, and we con-

clude that this transformation does not change the correlator. Then $I^R_{BA}(t) = i\theta(t)[I^T_{BA}(t) - (I^T_{BA}(t))^*]$, and we find

$$I^R_{BA}(t) = -2\theta(t)\mathrm{Im} I^T_{BA}(t). \tag{93}$$

Appendix D. Evaluation of conductivity in Eqs. (42) and (43)

To find the absorption power of electromagnetic field we need to calculate $\mathrm{Re}(\sigma_\omega)$, where the conductivity is given by Eq. (36) in the main text.

The integral in Eq. (36) is

$$\sigma_\omega = \mathcal{A}\int_{-\infty}^{\infty} dx \int_{-\infty}^{\infty} e^{i(\omega t - qx)}\,[K(t+i\delta) - K(t-i\delta)]dt, \tag{94}$$

$$K(t) = \frac{1}{(x-v_c t)^\lambda (x+v_c t)^\mu (x-v_s t)^\nu}, \tag{95}$$

where

$$\mathcal{A} = \frac{\left(eg\mu_B B_\perp\right)^2 a_0^{\lambda+\mu+\nu-2}}{\pi^2 p_F^3 \alpha}.$$

Since q is positive, the exponent e^{-iqx} vanishes at large x in the lower half-plane of the complex variable x. Therefore, the integral over real axis x is equal to the sum of two contour integrals in the lower half-plane of x along contours winding around two branch cuts shown in Fig. 6. The contour C_1 winds around the branch cut from the point $x = v_s t - i\delta$ to $x = +\infty - i\delta$, and the contour C_2 winds around the branch cut from $x = v_c t - i\delta'$ to $x = +\infty - i\delta'$. (We ignore here the potential singularity at $x = -v_c t$ which is associated with the inverse processes of spin flip from up to down on the right branch. These processes should be suppressed in the approximation of small excited-state occupation numbers which we employ.) We can estimate the integrals over x around each branch cut separately. The conductivity σ_ω has two singularities: at $\omega = v_s q$ and at $\omega = v_c q$. As we show below,

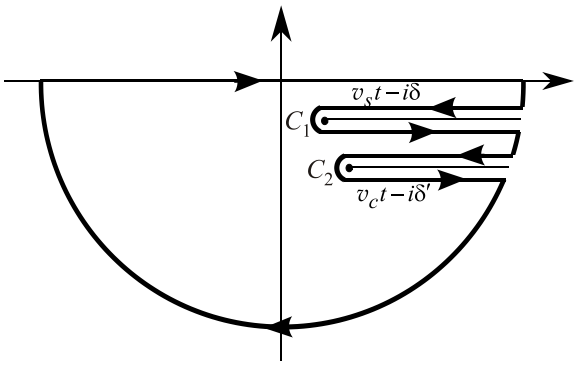

Fig. 6. The integration contour in the lower half-plane of the complex variable x.

close to the singularity near $\omega = v_s q$ the main contribution to the integral comes from contour C_1, and the other (plasmon) singularity is dominated by the integral over C_2.

First, we estimate the integral I_1 over the contour C_1. After the change of variable $u = x - v_s t$ the contour that maps C_1 in a complex plane u winds around the branch cut from $u = 0$ to $u = +\infty$ and will be denoted by the same symbol C_1. Thus, the integral I_1 can be written as follows:

$$I_1 = \int_{C_1} du\, \frac{e^{-iqu - iv_s qt}}{u^\nu \left[u + (v_s - v_c)t\right]^\lambda \left[u + (v_s + v_c)t\right]^\mu}.$$

We aim to approximate σ_ω very close to the resonance at $\omega_{\mathrm{res}} = v_s q$. The closeness is determined by inequalities relating to the detuning $\delta\omega = |\omega - \omega_{\mathrm{res}}|$:

$$\gamma << \delta\omega << \omega_{\mathrm{res}},$$

where γ is the attenuation rate mainly due to Cherenkov emission of phonons [13]. Then the time during which the resonance absorption is accumulated is large enough, $t \sim 1/\delta\omega$. In this limit, $(v_c - v_s)qt >> 1$, we approximate the above integral as

$$I_1 = \frac{e^{-iv_s qt}(-iq)^{\nu-1}}{\left[(v_s - v_c)t\right]^\lambda \left[(v_s + v_c)t\right]^\mu} \int_C z^{-\nu} e^z dz, \tag{96}$$

where we introduced new variable $z = -iqu$. As a result of this change of variables, the contour C_1 turns into contour C winding around a branch cut going from $z = 0$ to $z = -i\infty$. The contour C can be rotated clockwise together with the branch cut until the latter coincides with the left half of the real axis $z < 0$. Then the contour integral turns into the Hankel's representation of the inverse Gamma function and gives $2\pi i/\Gamma(\nu)$. After that we can integrate over time with the following final result:

$$I_{\omega,q} \simeq \mathcal{A}\frac{-2\pi i\Gamma(1-\lambda-\mu)q^{\nu-1} i^{-\nu-\lambda-\mu}}{(v_s - v_c)^\lambda (v_s + v_c)^\mu \Gamma(\nu)(\omega - v_s q + i\gamma)^{1-\lambda-\mu}}. \tag{97}$$

Then the real part of conductivity near $\omega = v_s q$ becomes

$$\mathrm{Re}\,\sigma_\omega \simeq \mathcal{A}\frac{\Gamma(1-\lambda-\mu)q^{\nu-1}}{(v_c - v_s)^\lambda (v_c + v_s)^\mu \Gamma(\nu)} \times$$

$$\times \frac{\gamma}{\left[(\omega - \omega_{\mathrm{res}})^2 + \gamma^2\right]^{1-\frac{\lambda+\mu}{2}}}, \tag{98}$$

which for small λ and μ is approximated by Eq. (42). Here we used that $v_c \geq v_s$. The integral I_2 over the contour C_2 does not contribute to the singularity at $\omega = v_s q$ and therefore can be neglected.

In addition, there is also a small part of $\mathrm{Re}\,\sigma_\omega$ which is independent of γ:

$$\frac{\pi^2 \mathcal{A}\Gamma(1-\lambda-\mu)q^{\nu-1}(\nu+\lambda+\mu-2)}{(v_c-v_s)^{\lambda}(v_c+v_s)^{\mu}\Gamma(\nu)\,|\,\omega-\omega_{res}\,|^{1-\lambda-\mu}}. \qquad (99)$$

It is small in positive parameter

$$\nu+\lambda+\mu-2=(\delta v)^2(K_c-1)^2/[4K_c(v_c+v_s)^2].$$

Nevertheless, I_2 contributes to a singularity at plasma frequency $\omega=v_cq$. Next we analyze this singularity. We consider the integral I_2 over contour C_2 similarly to what we did for I_1. We change variable in I_2 to $u=x-v_ct$. The mapped contour C_2 winds around the branch cut from $u=0$ to $u=+\infty$. As a result of winding around the branch cut we obtain factor $(1-\mathrm{e}^{-2\pi i(\lambda-1)})\approx 2\pi i\lambda$ and the integral over u from 0 to infinity:

$$I_2=2\pi i\lambda\int_0^{\infty} du\,\frac{\mathrm{e}^{-iq\left(u+v_ct\right)}}{u^{\lambda}\left(u+2v_ct\right)^{\mu}\left[u+(v_c-v_s)t\right]^{\nu}}. \qquad (100)$$

At small detuning $\delta\omega=|\,\omega-v_cq\,|$ from the plasma resonance we expect that similarly to what we observed for I_1 the accumulation time for the resonance absorption is large, $t\sim 1/\delta\omega>>1/(v_cq)$, and therefore in the factors $u+2v_ct$, $u+(v_c-v_s)t$ it is possible to neglect $u\sim 1/q$. After this procedure the resulting integral over t diverges at $t=0$. This divergence however is spurious. It has happened because at small $t<1/[(v_c-v_s)q]$, the variable u cannot be neglected. It means that the integration over t is effectively cut off at $t_0<1/[(v_c-v_s)q]$. To estimate the singular part on the background of nonsingular contribution originated from small t, we represent the exponent $\mathrm{e}^{i(\omega-v_cq)t}$ as a sum, $\mathrm{e}^{i(\omega-v_cq)t}=[\mathrm{e}^{i(\omega-v_cq)t}-1]+1$, and divide the integral over time into two parts:

$$\int_{t_0}^{\infty}\frac{\left[\mathrm{e}^{i(\omega-v_cq)t}-1\right]dt}{t^{\mu+\nu}}+\int_{t_0}^{\infty}\frac{dt}{t^{\mu+\nu}}.$$

The second integral is approximately equal to $t_0^{1-\mu-\nu}/(\nu+\mu-1)$ and has no singularity. The first integral converges and can be extended to $t=0$ if $\mu+\nu<2$. This condition is satisfied in a broad range of not too strong interaction as it can be readily checked from Eqs. (18)–(20). The first integral after the change of variable $\tau=(\omega-v_cq)t$ turns into

$$\left(\omega-v_cq\right)^{\mu+\nu-1}\int_0^{\infty}\frac{(e^{i\tau}-1)d\tau}{\tau^{\mu+\nu}}. \qquad (101)$$

The integral in Eq. (101) is a large number $\approx i(2-\mu-\nu)^{-1}$ proportional to $[\delta v/(v_c-v_s)]^{-2}$. The ratio of the first term to the second has the order of magnitude $[\delta v/(v_c-v_s)]^{-2}[|\,\omega-v_cq\,|/(v_cq)]^{\mu+\nu-1}$. Thus, the nonresonant contribution is comparable with the resonant one only in a narrow region close to the resonance $\delta\omega\le v_cq[\delta v/(v_c-v_s)]^2$. Combining all the results, we arrive at the expression for the singularity due to spin-flip processes at the plasmon frequency:

$$I_{\omega,q}\simeq -\mathcal{A}i^{\lambda-1}q^{\lambda-1}\frac{2\pi\lambda\Gamma(1-\lambda)}{2-\mu-\nu}\frac{\left(\omega-v_cq+i\gamma\right)^{\mu+\nu-1}}{(2v_c)^{\mu}(v_c-v_s)^{\nu}}. \qquad (102)$$

The calculation of the real part gives the following result:

$$\mathrm{Re}\,I_{\omega,q}\simeq\mathcal{A}\frac{2\pi\lambda\Gamma(1-\lambda)q^{\lambda-1}}{\left(2v_c\right)^{\mu}(v_c-v_s)^{\nu}(2-\mu-\nu)}\times$$

$$\times\frac{\gamma}{\left[(\omega-v_cq)^2+\gamma^2\right]^{1-\frac{\mu+\nu}{2}}}, \qquad (103)$$

c.f. (43) in the main text for $\mathrm{Re}\,\sigma_\omega$. The plasmon singularity has a character of a weak cusp that can be detected only at large enough interaction.

Appendix E. Bosonization

The left and right chiral fermionic fields are expressed in terms of the bosonic fields as follows:

$$\Phi_{\sigma,\tau}=\frac{\eta_\sigma}{\sqrt{2\pi a_0}}\mathrm{e}^{i\sqrt{4\pi}\varphi_{\sigma,\tau}}, \qquad (104)$$

where η_σ are Klein factors (see Sec. 2) and Bose fields $\varphi_{\sigma,\tau}$ obey the following commutation relations valid for two operators of the Bose field at the same moment of time, but different positions:

$$\left[\varphi_{\sigma,\tau}(x),\varphi_{\sigma',\tau'}(y)\right]=\frac{i\tau}{4}\delta_{\sigma,\sigma'}\delta_{\tau,\tau'}\mathrm{sign}\,(x-y). \qquad (105)$$

Finally the Klein factors obey the following anticommutation and algebraic relations:

$$\left\{\eta_\sigma,\eta_{\sigma'}\right\}=2\delta_{\sigma,\sigma'};\;\;\eta_\sigma^{\dagger}=\eta_\sigma;\;\;\eta_+\eta_-=i. \qquad (106)$$

Appendix F. Spin-density correlations

Here we present calculations of the spin density correlations for the ordinary LL state. In terms of the bosonic fields, the spin-density operators reads

$$s_x(x)=\frac{1}{\pi a_0}\sin[\sqrt{2\pi}(\theta_s-\varphi_s)-2m\alpha x]+\frac{1}{\pi a_0}\sin[\sqrt{2\pi}(\theta_s+\varphi_s)-2m\alpha x]+$$

$$+\frac{1}{\pi a_0}\sin[\sqrt{2\pi}(\theta_s-\varphi_c)+(2k_F-2m\alpha)x]+\frac{1}{\pi a_0}\sin[\sqrt{2\pi}(\theta_s+\varphi_c)-(2k_F+2m\alpha)x],$$

$$s_y(x)=\frac{1}{\pi a_0}\cos[\sqrt{2\pi}(\theta_s-\varphi_s)-2m\alpha x]+\frac{1}{\pi a_0}\cos[\sqrt{2\pi}(\theta_s+\varphi_s)-2m\alpha x]+$$

$$+\frac{1}{\pi a_0}\cos[\sqrt{2\pi}(\theta_s-\varphi_c)+(2k_F-2m\alpha)x]+\frac{1}{\pi a_0}\cos[\sqrt{2\pi}(\theta_s+\varphi_c)-(2k_F+2m\alpha)x],$$

$$s_z(x)=-\sqrt{\frac{2}{\pi}}\partial_x\varphi_s(x)-\frac{1}{\pi a_0}\sin[\sqrt{2\pi}(\varphi_c-\varphi_s)+2k_Fx]+\frac{1}{\pi a_0}\sin[\sqrt{2\pi}(\varphi_c+\varphi_s)+2k_Fx]. \quad (107)$$

Let us define the partition function as a functional integral:

$$Z=\int\mathcal{D}\Phi(x,\tau)\exp\left[\int_0^\beta d\tau\int dx\mathcal{L}(\Phi(x,\tau))\right], \quad (108)$$

where $\tau=it+\varepsilon\,\mathrm{sgn}\,(t)(\varepsilon=0^+)$ is the imaginary time, $\beta=1/(k_BT)$, $\Phi=(\varphi_c,\theta_c,\varphi_s,\theta_s)$ is the four vector of fields, and $\mathcal{L}(\Phi(x,\tau))$ is the Lagrangian associated with the Hamiltonian H. Note that for the ordinary LL state H is completely quadratic and thus invariant under a uniform translation of any bosonic fields: $\Phi_i(x)\to\Phi_i(x)+A_i$, a symmetry which we use later. In the functional integral language, the time-ordered correlation for operators $A(\Phi)$ and $B(\Phi)$ is

$$\langle T_\tau A(\tau)B(0)\rangle=$$

$$=\frac{1}{Z}\int\mathcal{D}\Phi(x,\tau)A(\Phi(\tau))B(\Phi(0))\exp\left[\int_0^\beta d\tau\int dx\mathcal{L}(\Phi(x,\tau))\right]. \quad (109)$$

Later we will drop the time ordering symbol T_τ and use directly $\langle\rangle$ to denote the time-ordered average. The Lagrangian $\mathcal{L}$ can be written as

$$\mathcal{L}(\Phi)=-\frac{1}{2}\Phi M\Phi=\frac{1}{2}\Phi_iM_{ij}\Phi_j,$$

where the Fourier transform of the matrix $M(x,\tau)$ is

$$M(q,\omega)=\begin{pmatrix}\frac{v_cq^2}{K_c} & iq\omega & 0 & 0\\ iq\omega & v_cK_cq^2 & 0 & 0\\ 0 & 0 & \frac{v_sq^2}{K_s} & iq\omega\\ 0 & 0 & iq\omega & v_sK_sq^2\end{pmatrix}. \quad (110)$$

Note that here ω is the imaginary frequency associated with τ. The inverse of $M(q,\omega)$ reads

$$M^{-1}(q,\omega)=\begin{pmatrix}\frac{K_cv_c}{\Omega_c^2} & -\frac{i\omega}{q\Omega_c^2} & 0 & 0\\ -\frac{i\omega}{q\Omega_c^2} & \frac{v_c}{K_c\Omega_c^2} & 0 & 0\\ 0 & 0 & \frac{K_sv_s}{\Omega_s^2} & -\frac{i\omega}{q\Omega_s^2}\\ 0 & 0 & -\frac{i\omega}{q\Omega_s^2} & \frac{v_s}{K_s\Omega_s^2}\end{pmatrix}, \quad (111)$$

where we denoted $\Omega_{c/s}^2=v_{c/s}^2q^2+\omega^2$. Let $\Phi_i(q,\omega)$ be the Fourier transform of $\Phi_i(x,\tau)$. Then

$$\langle\Phi_i(q,\omega)\Phi_j(-q,-\omega)\rangle=\beta lM_{ij}^{-1}(q,\omega). \quad (112)$$

Correlations for $\varphi_{s/c}(x,\tau)$ and $\theta_{s/c}(x,\tau)$ can be obtained from Eq. (112) by inverse Fourier transform. The results at zero temperature are

$$\langle(\varphi_{s/c}(x,\tau)-\varphi_{s/c}(0,0))^2\rangle=\frac{K_{s/c}}{2\pi}\log\frac{x^2+y_{s/c}(\tau)^2}{a_0^2}, \quad (113a)$$

$$\langle(\theta_{s/c}(x,\tau)-\theta_{s/c}(0,0))^2\rangle=\frac{1}{2\pi K_{s/c}}\log\frac{x^2+y_{s/c}(\tau)^2}{a_0^2}, \quad (113b)$$

$$\langle\varphi_{s/c}(x,\tau)\theta_{s/c}(0,0)\rangle=-\frac{i}{2\pi}\mathrm{Arg}\,[y_{s/c}(\tau)+ix], \quad (113c)$$

where $y_{s/c}(\tau)=v_{s/c}\tau+a_0\mathrm{sgn}\,(\tau)$. The argument in Eq. (113c) is defined with a branch cut at $(-\infty,0]$.

When calculating the spin-density correlators $s_{aa}(x,t)$ employing Eq. (107), there appear terms of three types: (a) $\langle\partial_x\varphi_s(x,\tau)\partial_x\varphi_s(0,0)\rangle$, (b) $\langle\partial_x\varphi_s(x,\tau)e^{i\sum A_i\Phi_i(0,0)}\rangle$, and (c) $\langle e^{i\sum B_i\Phi_i(x,\tau)}e^{i\sum C_i\Phi_i(0,0)}\rangle$, where A_i,B_i,C_i are

numerical coefficients. For their calculation we employ the invariance of H and $\mathcal{L}$ under the uniform translation of Φ_i. For terms of type (b) with $A_i \neq 0$, the translation $\Phi_i \to \Phi_i + \pi / A_i$ changes the sign of the averaged value leaving the Lagrangian invariant. Thus, the average $\langle \partial_x \varphi_s(x,\tau) e^{i\sum A_i \Phi_i(0,0)} \rangle$ must be zero if at least one $A_i \neq 0$. For terms of type (c), a similar argument shows that $\langle e^{i\sum B_i \Phi_i(x,\tau)} e^{i\sum C_i \Phi_i(0,0)} \rangle = 0$ if at least one of the sums $B_i + C_i \neq 0$. As a result, $s_{zz}(x,\tau)$ reduces to

$$s_{zz}(x,\tau) = \frac{2}{\pi}\langle \partial_x \varphi_s(x,\tau)\partial_x \varphi_s(0,0)\rangle + \frac{1}{4\pi^2 a_0^2}[e^{i2k_F x}\langle e^{i\sqrt{2\pi}(\varphi_c(x,\tau)-\varphi_s(x,\tau))} e^{-i\sqrt{2\pi}(\varphi_c(0,0)-\varphi_s(0,0))}\rangle + \text{h.c.}] +$$

$$+ \frac{1}{4\pi^2 a_0^2}[e^{i2k_F x}\langle e^{i\sqrt{2\pi}(\varphi_c(x,\tau)+\varphi_s(x,\tau))} e^{-i\sqrt{2\pi}(\varphi_c(0,0)+\varphi_s(0,0))}\rangle + \text{h.c.}]. \quad (114)$$

From Eq. (113a) it follows that

$$\frac{2}{\pi}\langle \partial_x \varphi_s(x,\tau)\partial_x \varphi_s(0,0)\rangle =$$

$$= \frac{2}{\pi}\partial_x \partial_{x'}\langle -\frac{1}{2}(\varphi_s(x,\tau) - \varphi_s(x',0))^2\rangle|_{x'=0} =$$

$$= \frac{2}{\pi}\partial_x \partial_{x'}[-\frac{K_s}{4\pi}\log[\frac{(x-x')^2 + y_s(\tau)^2}{a_0^2}]]|_{x'=0} =$$

$$= \frac{K_s}{\pi^2}\frac{y_s^2 - x^2}{(x^2 + y_s^2)^2}. \quad (115)$$

In Eq. (115) we applied the formula $\langle e^{iA}\rangle = e^{-\frac{1}{2}\langle A^2\rangle}$ valid for any Gaussian distributed variable A. Let calculate for example an average:

$$\langle e^{i\sqrt{2\pi}(\varphi_c(x,\tau)-\varphi_s(x,\tau))} e^{-i\sqrt{2\pi}(\varphi_c(0,0)-\varphi_s(0,0))}\rangle =$$

$$= \langle e^{i\sqrt{2\pi}(\varphi_c(x,\tau)-\varphi_s(x,\tau))-i\sqrt{2\pi}(\varphi_c(0,0)-\varphi_s(0,0))}\rangle =$$

$$= e^{-\pi\langle[\varphi_c(x,\tau)-\varphi_s(x,\tau)-\varphi_c(0,0)+\varphi_s(0,0)]^2\rangle} =$$

$$= e^{-\pi[\frac{K_c}{2\pi}\log\frac{x^2+y_c(\tau)^2}{a_0^2} + \frac{K_s}{2\pi}\log\frac{x^2+y_s(\tau)^2}{a_0^2}]} =$$

$$= \left(\frac{a_0}{\sqrt{x^2+y_c^2}}\right)^{K_c}\left(\frac{a_0}{\sqrt{x^2+y_s^2}}\right)^{K_s}. \quad (116)$$

Similar calculations can be done for other terms in $s_{zz}(x,\tau)$ and for the other two spin density correlators, which lead to the results (7) in the main text. The z direction spin density correlators of the SDW state can also be calculated in the same way, with φ_s replaced by a constant that minimizes H_C.

Appendix G. Total spin correlations

We calculate the total spin correlators by integration the spin density correlators over coordinate. The integrals that must be evaluated are of the forms

$$I_1 = \int_{-\infty}^{\infty} d\tau \int_{-\infty}^{\infty} dx\, e^{i\omega\tau}\cos(kx)\frac{y_s^2 - x^2}{(x^2+y_s^2)^a},$$

$$I_2 = \int_{-\infty}^{\infty} d\tau \int_{-\infty}^{\infty} dx\, e^{i\omega\tau}\cos(kx)\frac{1}{(x^2+y_c^2)^b (x^2+y_s^2)^c},$$

$$I_3 = \int_{-\infty}^{\infty} d\tau \int_{-\infty}^{\infty} dx\, e^{i\omega\tau}\cos(kx)\frac{1}{(x^2+y_c^2)^d}, \quad (117)$$

where $k \geq 0$ and a, b, c, d are constants, and ω is imaginary frequency associated with τ. The integrals I_1 or I_2 are parts of the correlations with small q or $q \sim 2k_F$ of the ordinary LL state, and I_3 corresponds to the z-component total spin correlations of the SDW state.

The calculations are simpler in polar coordinates (r,φ) related in the standard way to cartesian coordinates: $x = r\cos\varphi$ and $y_s = r\sin\varphi$. For example, I_1 reads

$$I_1 = \frac{1}{v_s}\int_0^{2\pi} d\varphi \int_0^{\infty} dr\, e^{ir(k\cos\varphi + \frac{\omega}{v_s}\sin\varphi)}\frac{r^2(\sin^2\varphi - \cos^2\varphi)}{r^{2a-1}} =$$

$$= -\frac{1}{v_s}\int_0^{2\pi} d\varphi \int_0^{\infty} dr\, e^{ir\sqrt{k^2+\frac{\omega^2}{v_s^2}}\cos(\varphi - \arctan\frac{\omega}{kv_s})}\frac{\cos(2\varphi)}{r^{2a-3}} =$$

$$= \frac{\pi\Gamma(3-a)}{v_s\Gamma(a)}\frac{k^2v_s^2 - \omega^2}{k^2v_s^2 + \omega^2}\left(\frac{k^2v_s^2 + \omega^2}{4v_s^2}\right)^{a-2}. \quad (118)$$

The calculation of the integrals I_2, and also I_3 is similar, but for them the approximation $v_c = v_s = v_F$ is sufficient. The results are

$$I_2 = \frac{\pi\Gamma(1-b-c)}{v_F\Gamma(b+c)}\left(\frac{k^2v_F^2-\omega^2}{4v_F^2}\right)^{b+c-1},$$

$$I_3 = \frac{\pi\Gamma(1-d)}{v_c\Gamma(d)}\left(\frac{k^2v_c^2-\omega^2}{4v_c^2}\right)^{d-1}. \qquad (119)$$

Applying these results to the correlations and analytically continuing to real frequency by $i\omega \to \omega + i\delta$, we obtain the correlations for the ordinary LL state:

$$S^R_{xx}(\omega) = S^R_{yy}(\omega) =$$

$$= A_0(\omega_s^2+\omega^2)(\omega_s^2-\omega^2)^{\frac{K_s}{2}+\frac{1}{2K_s}-2} +$$

$$+\frac{1}{2}A^x_{2k_F}[(\omega_+^2-\omega^2)^{\frac{K_c}{2}+\frac{1}{2K_s}-1} + (\omega_-^2-\omega^2)^{\frac{K_c}{2}+\frac{1}{2K_s}-1}],$$

$$S^R_{zz}(\omega) = A^z_{2k_F}(\omega_0^2-\omega^2)^{\frac{K_c}{2}+\frac{1}{2K_s}-1}, \qquad (120)$$

and those for the SDW state:

$$S^R_{xx}(\omega) = S^R_{yy}(\omega) = 0, \quad S^R_{zz}(\omega) = A_{SDW}(\omega_{0c}^2-\omega^2)^{\frac{K_c}{2}-1}. \qquad (121)$$

In the latter two equations we have defined the frequencies $\omega_s = 2m\alpha v_s$, $\omega_0 = 2k_Fv_F$, $\omega_\pm = 2(k_F \pm m\alpha)v_F$, $\omega_{0c} = 2k_Fv_c$, and the amplitudes

$$A_0 = \frac{l(\frac{a_0}{2v_s})^{K_s+\frac{1}{K_s}-2}\Gamma(2-\frac{K_s}{2}-\frac{1}{2K_s})}{\pi v_s\Gamma(1+\frac{K_s}{2}+\frac{1}{2K_s})},$$

$$A^x_{2k_F} = \frac{l(\frac{a_0}{2v_F})^{K_c+\frac{1}{K_s}-2}\Gamma(1-\frac{K_c}{2}-\frac{1}{2K_s})}{\pi v_F\Gamma(\frac{K_c}{2}+\frac{1}{2K_s})},$$

$$A^z_{2k_F} = \frac{l(\frac{a_0}{2v_F})^{K_c+K_s-2}\Gamma(1-\frac{K_c}{2}-\frac{K_s}{2})}{\pi v_F\Gamma(\frac{K_c}{2}+\frac{K_s}{2})},$$

$$A_{SDW} = \frac{2l(\frac{a_0}{2v_c})^{K_c-2}\Gamma(1-\frac{K_c}{2})}{\pi v_c\Gamma(\frac{K_c}{2})}. \qquad (122)$$

In these equations ω is assumed to have a small imaginary part. Note that the expressions for the $q \sim 2k_F$ parts of the ordinary LL correlations are only approximations when v_c and v_s are both close to v_F.

We remind that the conservation of S_z requires that $S^R_{zz}(\omega) = 0$ at any ω in the absence of the transverse external magnetic field. In the main text we have demonstrated that this discrepancy is associated with the inconsistency of the LL model at negative, large by modulus k and how this discrepancy can be corrected.

1. Y. Wu, J. Xiang, C. Yang, W. Lu, and C. M. Lieber, *Nature* **430**, 61 (2004).
2. L.J. Lauhon, M.S. Gudiksen, and C.M. Lieber, *Philosophical Transactions of the Royal Society of London. Series A: Mathematical, Physical and Engineering Sciences* **362**, 1247 (2004).
3. S.-B. Kim, J.-R. Ro, K.-W. Park, and E.-H. Lee, *J. Crystal Growth* **201**–**202**, 828 (1999).
4. O. Zsebok, J.V. Thordson, B. Nilsson, and T.G. Andersson, *Nanotechnology* **12**, 32 (2001).
5. C.L. Zhang, Z.G. Wang, Y.H. Chen, C.X. Cui, B. Xu, P. Jin, and R.Y. Li, *Nanotechnology* **16**, 1379 (2005).
6. Y.L. Lin, S.C. Lee, S.Y. Lin, and J.Y. Chi, in *5th IEEE Conference on Nanotechnology* (2005), Vol. 1, pp. 407–409.
7. M.A. Verheijen, G. Immink, T.D. Smet, M.T. Borgstrom, and E.P.A.M. Bakkers, *J. Am. Chem. Soc.* **128**, 1353 (2006).
8. T. Schapers, J. Knobbe, and V.A. Guzenko, *Phys. Rev. B* **69**, 235323 (2004).
9. G. Dresselhaus, *Phys. Rev*. **100**, 580 (1955).
10. E.I. Rashba, *Sov. Phys. Solid State* **2** (1960)
11. Y.A. Bychkov and E.I. Rashba, *Pis'ma ZhETF* **66**, 66 (1984).
12. A. Shekhter, M. Khodas, and A.M. Finkelstein, *Phys. Rev. B* **71**, 165329 (2005).
13. Ar. Abanov, V.L. Pokrovsky, W.M. Saslow, and P. Zhou, *Phys. Rev. B* **85**, 085311 (2012).
14. O.A. Tretiakov, K.S. Tikhonov, and V.L. Pokrovsky, *Phys. Rev*. **88**, 125413 (2013).
15. T. Giamarchi, *Quantum Physics in One Dimension*. Claredon Press, Oxford (2003).
16. A.O. Gogolin, A.A. Nersesyan, and A.M. Tsvelik, *Bosonization and Strongly Correlated Systems*, Cambridge University Press, Cambridge (2004).
17. S.A. Crooker, D.G. Rickel, A.V. Balatsky, and D.L. Smith, *Nature (London)* **431**, 49 (2004).
18. J. Sun, S. Gangadharaiah, and O.A. Starykh, *Phys. Rev. Lett*. **98**, 126408 (2007); S. Gangadharaiah, J. Sun, and O.A. Starykh, *Phys. Rev. B* **78**, 054436 (2008).
19. E.I. Rashba and A.L. Efros, *Phys. Rev. Lett*. **91**, 126405 (2003).
20. p_y and p_z are neglected, as the transverse motion is quantized, so $\mathbf{B}_{so} = (\alpha p, \beta p, 0)$.
21. P. Upadhyaya, S. Pramanik, and S. Bandyopadhyay, *Phys. Rev. B* **77**, 045306 (2006).
22. E.I. Ivchenko and G.E. Pikus, *Sov. Phys. JETP Lett*. **27**, 604 (1978).

23. V. Belinicher, *Phys. Lett. A* **66**, 213 (1978).
24. S. Ganichev and W. Prettl, *J. Phys: Condens. Matter* **15**, R935 (2003).
25. S. Tarasenko and E. Ivchenko, *JETP Lett*. **81**, 231 (2005).
26. S.D. Ganichev, S.N. Danilov, V.V. Belenicher, S. Giglberger, S.A. Tarasenko, E.L. Ivchenko, D. Weiss, W. Jantsch, F. Schaffler, D. Gruber, and W. Prettll, *Phys. Rev. B* **75**, 155317 (2007).
27. M.I. Dyakonov and V.I. Perel, *Sov. Phys. JETP* **33**, 1053 (1971).
28. M.I. Dyakonov, *Basics of Semiconductor and Spin Physics*, Chapter 1, in: *Spin Physics in Semiconductors*, Springer, New York (2008).
29. A.A. Kiselev and K.W. Kim, *Phys. Rev. B* **61**, 13115 (2000).
30. For simplicity we neglect the anisotropy of the g factor. Experimentally it is not small and must be accounted for in a more accurate theory.
31. M.V. Dorokhin, Y.A. Danilov, P.B. Demina, V.D. Kulakovskii, O.V. Vikhrova, S.V. Zaitsev, and B.N. Zvonkov, *J. Phys. D: Appl. Phys*. **41**, 245110 (2008).
32. R. Danneau, O. Klochan, W.R. Clarke, L.H. Ho, A.P. Micolich, M.Y. Simmons, A.R. Hamilton, M. Pepper, D.A. Ritchie, and U. Zulicke, *Phys. Rev. Lett.* **97**, 026403 (2006).
33. *Terahertz Sources and Systems*, R.E. Miles, P. Harrison, and D. Lippens (eds.), NATO Science Series, Ser. II, Vol. 27 Dordrecht: Kluwer Acad. Publ (2001).
34. A. Deninger and T. Renner, *Laser Focus World* **44**, 111 (2008).
35. M. Sherwin, *Nature* **420**, 131 (2002).
36. G.L. Carr, M.C. Martin, W.R. McKinney, K. Jordan, G.R. Neil, and G.P. Williams, *Nature* **420**, 153 (2002).
37. M.C. Hoffmann, J. Hebling, H.Y. Hwang, K.-L. Yeh, and K.A. Nelson, *J. Opt. Soc. Am. B* **26**, A29 (2009).
38. S.K. Singh and B.D. McCombe, *Phys. Rev. B* **58**, 7286 (1998) Also see the website http://sbfel3.ucsb.edu
39. S. Yamada, *Science and Technology of Advanced Materials* **6**, 406 (2005).
40. T. Sugaya, J.P. Bird, D.K. Ferry, A. Sergeev, V. Mitin, K.-Y. Jang, M. Ogura, and Y. Sugiyama, *Appl. Phys. Lett*. **81**, 727 (2002).
41. A.V. Moroz and C.H.W. Barnes, *Phys. Rev. B* **60**, 14272 (1999).
42. A.V. Moroz, K.V. Samokhin, and C.H.W. Barnes, *Phys. Rev. B* **62**, 16900 (2000).
43. M. Pustilnik, M. Khodas, A. Kamenev, and L.I. Glazman, *Phys. Rev. Lett.* **96**, 196405 (2006).
44. M. Khodas, M. Pustilnik, A. Kamenev, and L.I. Glazman, P*hys. Rev. B* **76**, 155402 (2007).
45. A. Imambekov and L.I. Glazman, *Science* **323**, 228 (2009).
46. R.G. Pereira and E. Sela, *Phys. Rev. B* **82**, 115324 (2010).
47. T.L. Schmidt, A. Imambekov, and L.I. Glazman, *Phys. Rev. Lett*. **104**, 116403 (2010).
48. T.L. Schmidt, A. Imambekov, and L.I. Glazman, *Phys. Rev. B* **82**, 245104 (2010).
49. V. Gritsev, G.I. Japaridze, M. Pletyukhov, and D. Baeriswyl, *Phys. Rev. Lett*. **94**, 137207 (2005).
50. L.D. Landau and E.M. Lifshitz, *The Classical Theory of Fields*, Fourth ed., Butterworth-Heinemann, Oxford (2004).
51. We retain the same notations $\psi_{R,\sigma}$ for the transformed fermionic operators.
52. A.A. Abrikosov, L.P. Gor'kov and I.Ye. Dzyaloshinskii, *Quantum Field Theoretical Method in Statistical Physics*, Pergamon, Oxford (1965).
53. They are presented here up to the quadratic order in small $\delta v/v_F$. There is also a contribution $\sim (x+v_s t)^{-\beta}$ in Eq. (36), but its exponent $\beta \sim (\delta v)^4$ is small and can be neglected to order $(\delta v)^2$.
54. This result corresponds to the case of interaction constant g_0 larger than $\delta v/v_F$.
55. S.A. Crooker, J. Brandt, C. Sandfort, A. Greilich, D.R. Yakovlev, D. Reuter, A.D. Wieck, and M. Bayer, *Phys. Rev. Lett*. **104**, 036601 (2010); Y. Li, N. Sinitsyn, D.L. Smith, D. Reuter, A.D. Wieck, D.R. Yakovlev, M. Bayer, and S.A. Crooker, *Phys. Rev. Lett*. **108**, 186603 (2012).
56. J. Hubner, R. Dahbashi, F. Berski, J. Wiegand, H. Kuhn, J. Lonnemann, and M. Oestreich, *Proc. SPIE* **9167**, 91672R (2014).
57. D.A. Tennant, R.A. Cowley, S.E. Nagler, and A.M. Tsvelik, *Phys. Rev. B* **52**, 13368 (1995).